JANUARY 2018

M.Sc. in Civil Engineering

AMER IBRAHIM HASSAN ZEBARI

UNIVERSITY OF GAZİANTEP

GRADUATE SCHOOL OF

NATURAL & APPLIED SCIENCES

INVESTIGATION OF DESIGN PARAMETERS EFFECTS PERFORMANCE OF CONCRETE FILLED STEEL COMPOSITE RECTANGULAR MEMBERS ACCORDING TO DESIGN CODES

M. Sc. THESIS

IN

CIVIL ENGINEERING

BY

AMER IBRAHIM HASSAN ZEBARI

JANUARY 2018

Investigation of Design Parameters Effects Performance of Concrete Filled Steel Composite Rectangular Members According to Design Codes

M.Sc. Thesis

in

Civil Engineering

Gaziantep University

Supervisor

Assist. Prof. Dr. Mehmet Tolga GÖĞÜŞ

by

Amer Ibrahim Hassan ZEBARI

January 2018

REPUBLIC OF TURKEY
UNIVERSITY OF GAZİANTEP
GRADUATE SCHOOL OF NATURAL & APPLIED SCIENCES
CIVIL ENGINEERING DEPARTMENT

Name of the thesis: Investigation of Design Parameters Effects Performance of Concrete Filled Steel Composite Rectangular Members According to Design Codes

Name of the student: Amer Ibrahim Hassan ZEBARI

Exam date: 15.01.2018

Approval of the Graduate School of Natural and Applied Sciences

Prof. Dr. Ahmet Necmeddin YAZICI
Director

I certify that this thesis satisfies all the requirements as a thesis for the degree of Master of Science.

Prof. Dr. Hanifi CANAKÇI
Head of Department

This is to certify that we have read this thesis and that in our consensus opinion it is fully adequate, in scope and quality, as a thesis for the degree of Master of Science.

Assist. Prof. Dr. Mehmet Tolga GÖĞÜŞ
Supervisor

Examining Committee Members:	Signature
Assist. Prof. Dr. Hasan Erhan YÜCEL	.....
Assist. Prof. Dr. Mehmet Tolga GÖĞÜŞ	.....
Assist. Prof. Dr. Talha EKMEKYAPAR	.....

I hereby declare that all information in this document has been obtained and presented in accordance with academic rules and ethical conduct. I also declare that, as required by these rules and conduct, I have fully cited and referenced all material and results that are not original to this work.

Amer Ibrahim Hassan ZEBARI

ABSTRACT

INVESTIGATION OF DESIGN PARAMETERS EFFECTS PERFORMANCE OF CONCRETE FILLED STEEL COMPOSITE RECTANGULAR MEMBERS ACCORDING TO DESIGN CODES

ZEBARI, Amer Ibrahim Hassan
M.Sc. in Civil Engineering
Supervisor: Assist. Prof. Dr. Mehmet Tolga GÖĞÜŞ
January 2018
62 pages

Rectangular Concrete Filled Steel Tube (RCFST) members are used widely around the world in various types of structures such as (building, bridges, and, towers etc.). RCFST members are classified according to AISC360-10 as compact, non-compact and slender based on the slenderness ratio (width-to-thickness b/t ratio) of the steel tube walls. In this thesis presents an investigation on a design which parameters affect the performance of RCFST members. There are several factors that affect the design of RCFST members. Other than the interaction between the steel and the concrete core, geometric and material properties like height of rectangular HSS member (H), width (B), thickness of the tube (t), yield strength of steel (f_y) and compressive strength of concrete (f_c'). Since the goal of the parametric study is to evaluate the contribution of the concrete, steel and dimensions quantitatively, the relative area and strength proportions of concrete to steel constitute the main parameters. The axial compression, and, flexural strength calculation basis of the applied calculation formula specification according to American Institute of Steel Construction (AISC360-10) and Eurocode 4 (EC4-2004) codes for the design of which parameter effects performance of RCFST members.

Keywords: Rectangular CFST members, Axial strength, Flexural strength, Design codes.

ÖZET

BETON DOLGULU ÇELIK KOMPOZIT DIKDÖRTGEN ÜYELER PERFORMANSINI ETKILEYEN PARAMETRELERIN TASARIM KODLARINA GÖRE INCELENMESI

ZEBARI, Amer Ibrahim Hassan
Yüksek Lisans Tezi, İnşaat Mühendisliği Bölümü
Danışman: Yard. Doç. Dr. Mehmet Tolga GÖĞÜŞ
Ocak 2018
62 sayfa

Dikdörtgen Beton Doldurulmuş Çelik Tüp (DBDÇT) elemanlar, çeşitli yapı türlerinde (bina, köprüler ve kuleler vb.) Dünyada yaygın şekilde kullanılmaktadır. DBDÇT elemanlar, çelik tüp cidarlarının narinlik oranına (genişlik-kalınlık b/t oranı) bağlı olarak AISC360-10'a göre kompakt, kompakt olmayan ve narin olarak sınıflandırılmıştır. Bu tezde DBDÇT elemanların performansını etkileyen parametrelerin araştırıldığı bir çalışma sunulmuştur. DBDÇT elemanlarının tasarımını etkileyen çeşitli faktörler vardır. Çelik ile beton çekirdeğin arasındaki etkileşimin yanı sıra, dikdörtgen HSS elemanının yüksekliği (H), genişliği (B), tüpün et kalınlığı (t), çeliğin dayanım kuvveti (f_y) ve beton basınç dayanımı (f_c') gibi geometrik ve malzeme özellikleridir. Parametrik çalışmanın amacı, beton, çelik ve boyutların nicel olarak katkısını değerlendirmek olduğundan, betonun çeliğe göreli alan ve dayanım oranlarıda ana parametreleri oluşturmaktadır. RCFST üyelerinin performansını hangi parametrenin etkilediğini tasarım için AISC360-10 ve EC4-2004 kodlarına göre uygulanan hesaplama formülünün eksenel basınç ve eğilme dayanımı hesabı esas alınmıştır.

Anahtar Kelimeler: Dikdörtgen DBDÇT elemanlar, Eksenel dayanım, Eğilme dayanımı, Tasarım kodları.

To

My Parents

My Beloved Wife KHADIJA

ACKNOWLEDGEMENT

I would like to express my special appreciation and thanks to my supervisor Assist. Prof. Dr. Mehmet Tolga GÖĞÜŞ, for all his help, patience, valuable advice, always providing and guiding me in the right direction. I'm very grateful and proudest to work under his academic guidance.

Special thanks to my family. Words cannot express how grateful I am to my father spirit that his words lead me to get certificates and my mother for all of the sacrifices that have made on my behalf. Also to all my sisters. I am greatly indebted to my wife, for their strong encouragement during the years of my study.

TABLE OF CONTENTS

Page

LIST OF FIGURES

Page

LIST OF TABLES

Page

ABBREVIATIONS

RCFST	Rectangular Concrete Filled Steel Tube
AISC360-10	American Institute of Steel Construction 2010
EC4-2004	Euro Code 2004
HSS	Hollow Steel Section
GLM	General Linear Model
BS	British Standard
AIJ	Architectural Institute of Japan
AS	Australian Standard
LRFD	Load Resistance Factor Design
ASD	Allowable Stress Design

LIST OF SYMBOLS

Symbols according to AISC360-10

f_c'	Specified compressive strength of concrete (MPa)
F_y	Specified minimum yield stress of the steel (MPa)
E_c	Modulus of elasticity of concrete = $(0.043 w_c^{1.5}\sqrt{f_c'}, MPa)$
E_s	Modulus of elasticity of steel = (200000 MPa)
w_c	Weight of concrete per unit volume $(1500 \leq w_c \leq 2500\ kg/m^3)$
B	Width of rectangular HSS member (mm)
H	Height of rectangular HSS member (mm)
t	Wall thickness of HSS member (mm)
b_c	Base of an HSS rectangular concrete cross-section $(b_c = b - 2t)$
h_c	Depth of rectangular concrete cross-section $(h_c = h - 2t)$
r	Radius of gyration of the cross-section
A_s	Cross-sectional area of steel section (mm^2)
A_c	Area of concrete (mm^2)
I_s	Steel cross-section moment of inertia (mm^4)
I_c	Concrete cross-section moment of inertia (mm^4)
Z_s	Plastic section modulus of steel (mm^3)
Z_c	Plastic section modulus of concrete (mm^3)
P_n	Nominal compressive strength (N)
P_{no}	Nominal compressive strength of zero length (N)
P_e	Euler or elastic critical buckling load (N)
P_p	Nominal bearing strength (N)
P_y	Axial yield strength (N)
EI_{eff}	Effective stiffness of composite section $(N - mm^2)$
F_{cr}	Critical stress (MPa)

k	Effective length factor
L	laterally unbraced length of the member (mm)
λ	Slenderness parameter
λ_p	Limiting slenderness parameter for compact element
λ_r	Limiting slenderness parameter for non-compact element
M_n	Nominal flexural strength $(N-mm)$
M_p	Plastic bending moment $(N-mm)$
M_y	Moment at yielding of the extreme fiber $(N-mm)$

Symbols according to EC4-2004

f_{cd}	Design value of cylinder compressive strength of concrete (MPa)
f_{ck}	Characteristic value of the cylinder compressive strength of concrete at 28 days (MPa)
f_{yd}	Design value of the yield strength of structural steel (MPa)
f_y	Nominal value of the yield strength of structural steel (MPa)
E_a	Modulus of elasticity of structural steel =210000 N/mm^2
E_{cm}	Secant modulus of elasticity of concrete (MPa)
A_a	Cross-sectional area of the structural steel section (mm^2)
A_c	Cross-sectional area of concrete (mm^2)
I_a	Second moment of area of the structural steel section (mm^4)
I_c	Second moment of area of the un-cracked concrete section (mm^4)
$M_{pI,Rd}$	Design value of the plastic resistance moment of the composite section $(N-mm)$
$N_{pI,Rd}$	Design value of the plastic resistance of the composite section to compressive normal force (N)
$N_{pI,Rk}$	Characteristic value of the plastic resistance of the composite section to compressive normal force (N)
N_{cr}	Elastic critical normal force (N)
χ	Reduction factor for flexural buckling
δ	Factor; steel contribution ratio; central deflection
$\bar{\lambda}$	Relative slenderness

CHAPTER 1

INTRODUCTION

1.1 General

One of the important decisions confronted by structural designers is the choice of materials used in civil engineering work. This decision is often based on structural and economic reasons and is backed by designer judgment and experience. The central goal is to achieve economic structure with outstanding performance.

The two materials widely used in civil engineering work are concrete and steel. The advantages of both materials are well known. Concrete is very hard, inexpensive and has good fire resistance. On the other hand, steel is strong, ductile and lightweight. The "smart" combination, or synergy, of these two materials results in a system with a much higher efficiency than the efficiency of the individual components. The name given to such a system includes the term hybrid, mixed or composite structure. Composite systems are successfully used for columns, beams and slabs in middle and high rise buildings, as well as bridges.

Recently, there was a wide application of composite materials, this is due to their great advantages. Concrete Filled Steel Tube (CFST) member system has been successfully used as a composite material system, claiming high strength, rigidity, ductility and earthquake resistance of the CFST member system. The main concept of CFST member system is that steel tubes and filled concrete of CFST member system can cover the most serious drawback of each material. Unconstrained concrete has poor deformability, shows very fracture rupture after maximum strength, and the strength of the steel member sharply decreases after local buckling (Choi K. K., 2007). The long term effects on composite column manifest themselves more significantly in the case of slender columns and columns with large concrete area (Grauers, 1993). For rectangular CFST and circular CFST columns, the concrete is well protected from shrinkage since it is

placed inside the concrete core. As shown in Figure 1.1, three main types of composite beam-columns are commonly used in the construction industry. Steel-encased concrete, CFST columns are constructed by pouring concrete into a rectangular or circular steel tubes called a RCFST and circular CFST, respectively (Tort and Hajjar, 2007).

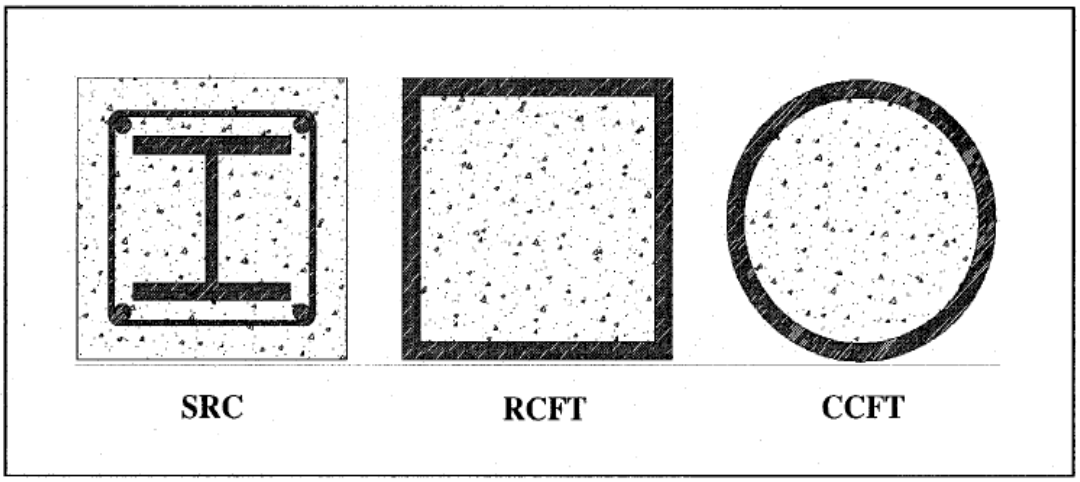

Figure 1.1 Typical composite CFST types (Tort and Hajjar, 2007).

1.2 Advantages of CFST members

CFST members have many advantages over both reinforced concrete and regular steel systems. Generally, the advantages are described as follows:

a) Interaction between steel tube and concrete:

- The occurrence of local buckling of the steel tube is delayed due to the restraining effect of the concrete, and the decrease in strength after the local buckling is alleviated.
- The strength of the concrete increases because of the confinement effect given by the steel tube. As the concrete sparing is prevented by the tube, the deterioration of strength is not very strict.
- The creep and dry shrinkage of concrete is greatly less than ordinary reinforced concrete.

b) The properties of the cross-sectional:

- The ratio of the steel in the CFST cross-section is greatly more than the steel ratio in the enclosed tube cross section and the reinforced concrete.
- Steel in the CFST section is located outside the section, so it is fully plasticized under bending.

c) Construction efficiency:

- The shape and reinforcement rod are omitted, concrete casting by tenure tube and pump-up method is done, which saves labor cost, construction cost and construction period.
- The construction site remains spotless.

d) Fire resistance

- Concrete improves fire performance, can reduce the amount of refractory material used, or omit its use.

e) Cost performance

- For the above benefits, better cost performance can be achieved by taking the place of the steel with CFST construction.

f) Ecology

- By omitting the form work and recycling steel tube and high concrete as recycled aggregate, we can reduce environmental burden.

1.3 Applications of CFST members

- CFST members are greatly used throughout the world in many types of structures. For instance, as shown in Figure 1.2, CFST members are used as columns of compound brace frames.

(a) (b)

Figure 1.2 (a) The Two Union Square building, Washington. (b) Cassel den Place project in Melbourne, Australia (Lai and Zhang, 2014).

- CFST members are used as compression chords in composite bridges, for example, in: as shown in Figure 1.3.

(a) (b)

Figure 1.3 (a) The Xialaoxi bridge in Yichang, China. (b) Jinan East Railway Station bridge in Jinan, China (Lai and Zhang, 2014).

1.4 Objectives of the thesis

Generally, the objective of the work is to study the parameters which have an effect on the design of Rectangular Concrete Filled Steel Tube (RCFST) members and also comparison of design codes. study the effect of parameters on the design of RCFST members.

- Compare the design codes including American Institute of Steel Construction (AISC360-10) and European Code (EC4-2004) for the purpose of calculating axial load and bending moment capacity for rectangular CFST.

- Therefore, the research will aim to:

1. Develop a spread sheet in order to determine both axial load and bending moment capacity of RCFST members.

2. Verify and compare the obtained results with the previous studies.

3. Study the impact of tested parameters on both axial load and bending moment capacity by using general linear model method.

4. Find which parameters has greater impact on both axial load and bending moment capacity.

1.5 Outline of the thesis

Consists of five Chapter summary and the division of each chapter as follows:

Chapter 1. Introduction:

The intention and scope of the thesis was presented.

Chapter 2. Literature review:

Previous studies based on the scope of the study were reviewed and maintained. Review of CFST literature and general background, parameters affecting the performance of RCFST on the axial load and bending moment capacities.

Chapter 3. Design concept:

In this Chapter, design of CFST structure by AISC360-10 and design of the composite concrete and steel structure in EC4-2004 Part2. These methods are used in the calculation of Chapter 4 on the bending moment and axial load capacity.

Chapter 4. Results and discussion:

In this Chapter, the results of the spread sheet used to calculate the axial load and bending moment capacity and verification results will be provided, also the results obtained by using general linear model method to determine the effect of parameters will be given.

Chapter 5. Conclusions:

Provide conclusions and summary based on the results of comparative investigations of this study.

CHAPTER 2

LITERATURE REVIEW

2.1 Parameters That Affecting the Performance Behavior of CFST Members

In this section, reviews the general behavior of CFST at the section level on the main parameters. The reviews summarized here relate mainly to materials of normal strength (steel and concrete), unless otherwise stated.

2.1.1 Local buckling

There are many advantages of CFST, the most important one is to delay the local buckling of steel tubes, which lead to a great deformation bulk. It's considered as an important standard for seismic performance of columns. The researchers agreed that the CFST members will greatly improve the ductility of the members. The reason of this deformability is that the existing concrete in the tube will lead to delay the local buckling.

As shown in Figure 2.1 by changing the deformation mode, the concrete will delay the local buckling of the steel tube. The Hollow Steel Section (HSS) fails due to inward buckling of the two sides and outward buckling of the other two sides. nonetheless, due to the presence of concrete, buckling inward of the CFST part is prevented, great strain is generated compared to the hollow sections, and excellent deformability is obtained. This local buckling delay increases ductility (Choi Y. H., 2004).

Lu and Kennedy (1994) performed pure beam tests which are done to study the bending CFST members of behavior, with respect to different ratios of steel and concrete, and different ratios of shear span-depth. Two points loadings were applied to both rectangular and square HSS and CFST sections made of normal strength material without any mechanical anchorage. The moment curvature relationship of the CFST beam was initially linear around 25% of the maximum moment, then followed by the increasing inelastic behavior and finally by a long plateau of little increase in

moment till failure occurred. The general failure mode of the hollow steel beam was downward (or inward) buckling of the upper flange, but the CFST beam failed by upward (or outward) buckling of the upper flange due to a filled concrete. The filled concrete also significantly improved the rotational capacity and the maximum curvature of the CFST section which is around three times more than that of the hollow steel section. This is due to the fact, that filled concrete, the steel in CFST beam was able to suffer larger strains before buckling occurred. It is also noticed the ratio of the shear span-depth does not influence the moment-curvature diagram. While a slight amount of slip between concrete and steel was observed before the maximum moment, no degradation in moment capacity was observed because of load transfer problems without mechanical port. The maximum curvature and the rotational capacity of the CFST beam is about three times with of the hollow steel beam.

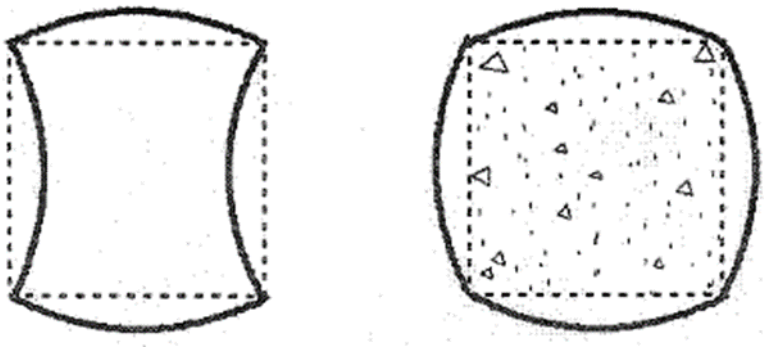

(a) Hollow section (b) CFST section

Figure 2.1 Deformation modes (Choi Y. H., 2004).

Zhang and Shahrooz (1999) performed two sets of fiber analysis on CFST beam-columns to examine the impact of local buckling. The first set of stress-strain relationships has the same compression and tension relationship and takes strain hardening into account. The second set has the same association as the first set for the tension, but has an elastoplastic relationship for compression to indirectly account for the effect of local buckling. The modeling methods limited the contribution to the yield strength of the compression steel fibers. From this analysis, it was found that the moment-curvature relationships from the two different analyses were correlated reasonably well with experimental results. The analysis results showed a slight difference with a large curvature after developing the maximum moment, but almost

the same behavior until it reached the maximum moment. The authors concluded that monotonicity strength was not greatly influenced by local buckling.

2.1.2 Confinement effect

Furlong (1967) presented one important factor about how much confinement can be achieved with a CFST columns is the ratio of width-thickness (B/t) of a rectangular section steel tube or the ratio of diameter-thickness (D/t) of a circular part. The confinement influence is the result of suppressing the pressure on the concrete core of the steel tube, causing a concrete to under triaxial stress state. Thus, when the steel tube is more weakly to control the expansion of concrete in lateral direction, it is impossible to obtain the confinement effect. It is necessary for steel tubes to have stiffness enough to confine the side deformation of a concrete demand to obtain confinement effect. Figure 2.2 shows the load-strain relationship of two CFST members with different D/t "LOAD ON STEEL" in the Figure 2.2 is obtained by multiplying the area of steel tube due to the measured stress from a compression tests on a plain steel tube section, "TOTAL LOAD" represents measured value from the tests on CFST columns, and "LOAD ON CONCRETE" is calculated algebraically by subtracting "LOAD ON STEEL" from "TOTAL LOAD". In the part with D/t of 36 (the part with higher rigidity section), the strength of concrete increases after important strain achieved because of the confinement influence, whereas a section with D/t of 98 (weak part) fails without any increase of strength.

MacGregor (1992) investigated another distinct feature for CFST columns is the confinement provided by a steel tube to a concrete core. Concrete of CFST column surrounded by steel tube is in triaxial stress state. The ductility and strength of concrete under triaxial compression loading increases with the degree of lateral confinement. Figure 2.3 shows the stress-strain curve of a concrete cylinder subjected to a constant lateral pressure ($\sigma_2 = \sigma_3$) and the longitudinal stress (σ_1) increased until failure. As the lateral pressure increases, the longitudinal strength and deformation ability also be increase. The longitudinal stress at fracture is given by the Eq. (2.1).

$$\sigma_1 = f_c' + 4.1\sigma_3 \tag{2.1}$$

However, confinement for CFST columns is a little different from that described above. At the same time, as a load is likely to act on a steel tube and a concrete core.

The steel tube that provides a confinement also undergoes a lateral deformation due to Poisson's ratio, and therefore it is not able to provide a perfect confinement, indicating that the confinement in the CFST members is not as effective as Eq. (2.1).

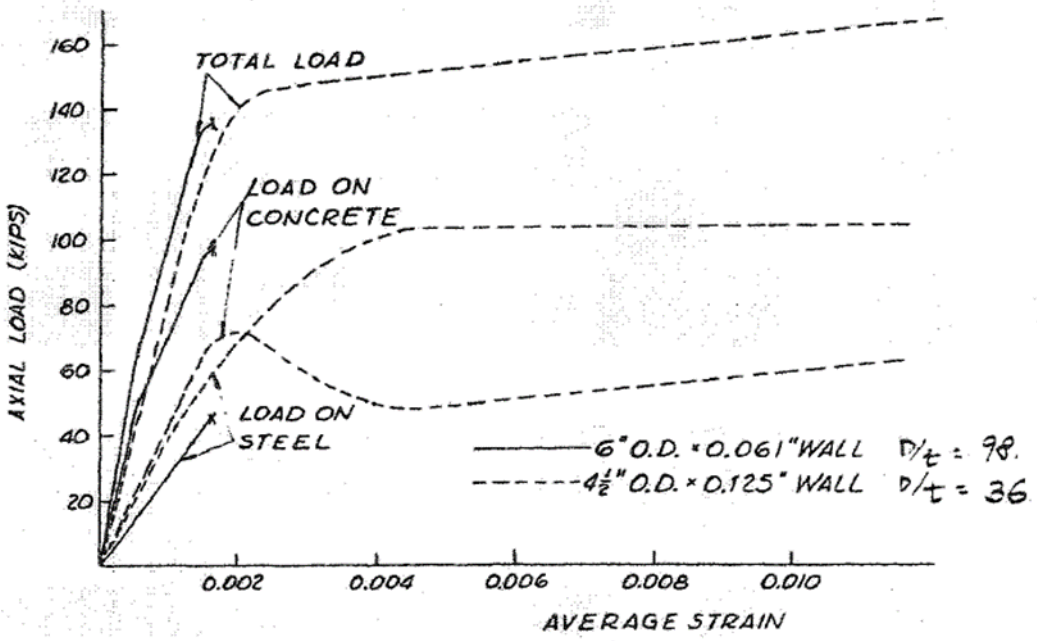

Figure 2.2 Load-strain relationship (Furlong, 1967).

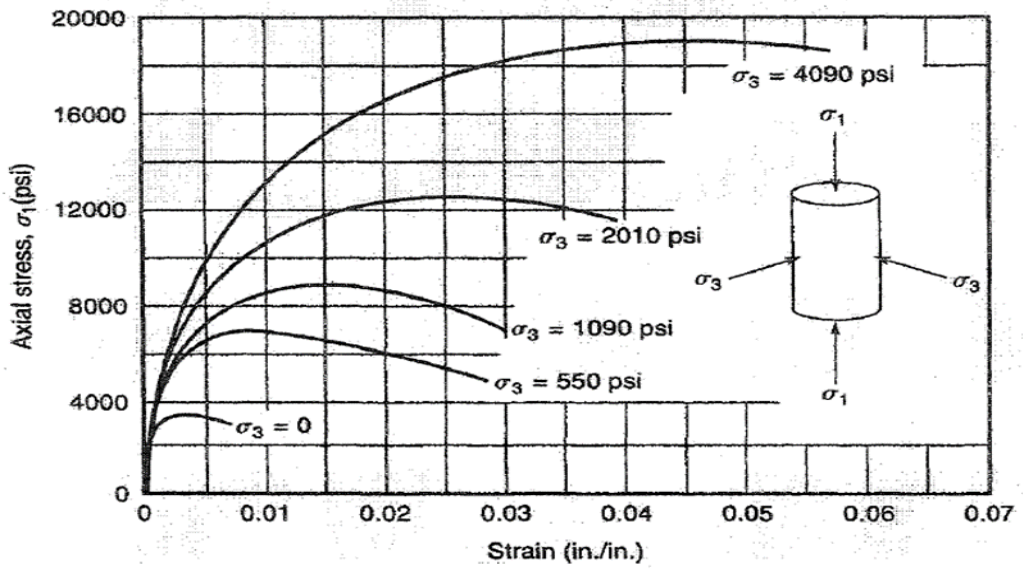

Figure 2.3 Axial stress-strain curves by triaxial compression tests (MacGregor, 1992).

2.1.3 Width-thickness (B/t) ratio

Gardner and Jacobson (1967) investigated 22 specimens of the composite columns with the ratio D/t between 30-40. These results showed that the steel tube with the ultimate load was at failure level while concrete core was not broken. However, an increased strain level was noticed for the steel tube without local buckling, showing that the concrete made the tube wall stable.

Tomii and Sakino (1979) investigated a strain-stress typical CFST columns of a concrete in square. In order to analytically evaluate the moment thrust curvature relation. Figure 2.4 shows a schematic model in which the post-peak response of concrete is highly related to the ratio of B/t of a steel part. The strength is the same for all ranges of B/t before strain of 0.005, but changes after strain of 0.005 depending on the ratio of B/t of steel tube. The strength maximum of concrete with steel tube ratio of width-thickness of 24 or less is always maintained even after 0.015 strain. Concrete strength at B/t greater than 64 begins to fall with a strain of 0.005 and no strain at 0.015 strain.

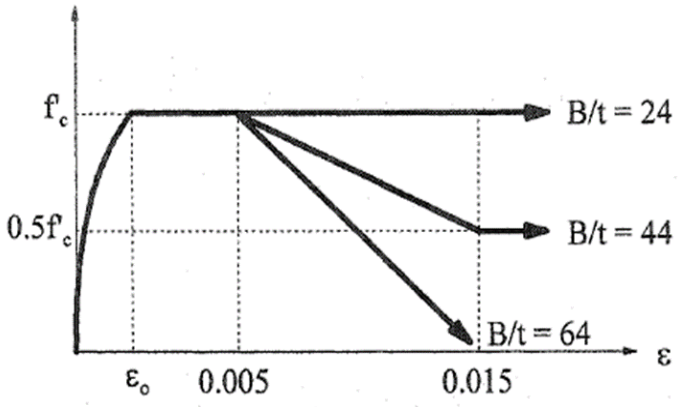

Figure 2.4 Concrete Model of CFST members (Tomii and Sakino, 1979).

Sakino et al. (1985) carried a tests for 18 circular samples, the D/t ratio of these samples was 18-192. Three samples were exposed to different types of loads. For the first sample group, the axial load was applied both steel tube and the concrete in the same time. A specific load was applied to the concrete core in the second sample group, it was similar to that of the third group, except the inside tube wall was greased before casting the concrete. The results showed that when the concrete core and the steel tube

were loaded at the same time, the tube provided no confinement until post yield behavior. In the specimens with only concrete, several longitudinal stresses were observed in the steel tube even for columns with walls with grease. Therefore, regardless of the loading condition, the wall of the steel tube appeared to be primarily in a biaxial stress state. Although test results showed that the axial nine rigidity of the concrete loaded only columns were about half that of the other CFST tested, but the concrete loaded only columns got a greater yield and ultimate axial load capacity.

Kang et al. (2001) carried out an analytical and experimental study on the behavior of concrete filled tubular stub columns concentrically loaded in compression to fail. A total of 11 specimens were tested and the test parameters are the depth-thickness ratio of the steel tube and the ratio of concrete cylinder strength-yield stress of steel tube. The ratio of the depth-thickness of steel tube between $20.22<B/t<91.75$, and the ratio of concrete cylinder strength-yield stress of steel tube between $0.0680< (f_{ck}/f_y) <0.0955$ were limited. Development of a polynomial equation for the cross-section strength of square concrete filled steel tube. This formula provides an accurate representation of the cross-section strength of a concentrically loaded CFST. This expression is verified against short term of the experimental tests.

Gupta et al. (2007) have done a computational and experimental studies regarding the behavior of the axial load capacity on the circular CFST columns. The computational analysis was done by using finite element method with ANSYS software, and the experimental campaign which comprised of 81 samples which were strongly loaded until failure. The major reason of developing nonlinear finite element model is to study the load holding mechanism of the CFST. Mainly four parameters were studied including, diameter-thickness ratio (D/t), concrete grade, fly ash volume in the concrete mixture and the length-tube diameter ratio (L/D). When the different outer diameters and steel thicknesses were used, the ratio of D/t between 25 to 39. For casting of the concrete of CFST specimens, 30 MPa and 40 MPa the design strengths were used. It was noticed that, the confinement effect of the concrete infill decreases as the concrete strength increases. Also, by the increase of fly ash up to 20-25 % the energy absorbing capacity at a given deformation decreases. Furthermore, the load slope against verses deformation curves of the experimental data is smaller than the slope of the analytical model.

2.1.4 Concrete strength

Knowles and Park (1969) studied seven square and 12 circulars columns with D/t ratios of 15, 22 and 59, and L/D ratios ranging from 2 to 21. The results showed that the tangent modulus method accurately predicted the capacity of the columns with L/D ratios greater than 11, but was slightly conservative in columns with small slenderness ratios. It was concluded that this capacity larger than expected capacity for composite columns with L/D < 11 was due to the increase of concrete strength resulting from triaxial confinement effects. It has been observed that for certain values of longitudinal strain the concrete began to increase in volume due to micro cracks, which induced concrete confinement by the steel tube. This confinement improved the overall load-resisting capacity of the CFST column.

O'Shea and Bridge (2000) developed a design method that can be used to conservatively evaluate the strength of circular CFST under several loading conditions. The loading conditions included axial loading of the concrete only, axial loading of the steel only and axial simultaneous axial loading of the steel concrete and along small eccentricities. The developed design method has been validated and calibrated based on recent tests on circular CFST. The infill of concrete nominal unconfined cylinder had strengths of 50 MPa, 80 MPa, and 120 MPa. The test samples were short with a diameter-thickness ratio (D/t) ranging between 60 and 220 and a length-diameter ratio (L/D) of 3.5. It was observed that the load carrying capacity of unfilled circular steel tubes is significantly influenced by local buckling. Although the buckling strength of square tubes can be improved by providing inside lateral restraint, this was not observed in the examined circular steel tubes. Instead, the mainly outward buckles were not affected by the internal concrete. Also, the loading condition greatly influences the degree of confinement provided by a thin walled circular steel tube to the concrete filling material. The maximum confinement occurred when the CFST was axially loaded with only the concrete loaded while the steel tube acted as pure circumferential restraint. Furthermore, if there is sufficient bond between the concrete and steel is present, local buckling of the confining steel tube does not occur. Therefore, the provisions of EC4-2004 can be used without reduction for local buckling if concrete infill strengths up to 80MPa. EC4-2004 can be used without reducing the steel strength from local buckling and biaxial effects and without

enhancing the infill concrete for confinement. Finally, the authors pointed out that the current simplified methods can give very unconservative strength estimates when used outside their calibrated range. In addition, EC4-2004 can use thin-walled steel tubes filled with only very high strength concrete if the design equations are formulated carefully.

A comprehensive experimental study was done by Mursi and Uy (2004) the study was about thin-walled steel sections which use high-strength steel with normal strength concrete. As it shown in Figure 2.5, a numerical model is greeted to examine the behavior of slender concrete with high steel column strength combining both geometric non-linarites and material. In this analysis, the stability of the member is investigated by the use an idealized stress-strain relation for both concrete material and the steel material based on elasticity and plasticity ranges. The experimental results of columns with high strength steel casings are used for comparison. The impact of confined concrete core is taken and the method shows mostly a similar results the experimental results of the compact sections of concrete filled steel columns.

Figure 2.5 Hollow and composite slender steel box columns (Mursi and Uy, 2004).

A study was carried out by Ellobody et al. (2006) the design of an axially loaded circular CFST stub columns were investigated by using a nonlinear finite element code ABAQUS. A wide range of concrete cube strengths ranging from 30 MPa to 110 MPa was used. The ratio of column diameter-steel thickness (D/t) was between 15 to 80.

By using the American, European, and Australian code, the predicted column strength was compared to the calculated design strength. In the case of an axial load CFST circular column, it was founded that the American and the Australian Specifications can provide reliable limit state design when examined with a resistance coefficient υ = 0.85. This study also indicated that the design strengths given in European standards are generally non-conservative, while the design strength when using American and Australian code are conservative.

An investigation study was done by Lu et al. (2007) on the axial load and bending moment curvature (M-N-ϕ) relative to eccentrically compressed of CFST square columns shown in Figure 2.6 was achieved by analysis of the dynamics incomes into reason the influence of remaining stress of steel and non-linearity of steel and concrete. A basic analytical method for expecting the ultimate strength of eccentrically compressed CFST square columns constructed on the collapse system. Since the suggested method can be also used for prediction the ultimate strength of the axial load columns with preliminary imperfections as they were treated as a corresponding somewhat eccentrically compressive of column. The suggested method agrees good with the experiments results obtained.

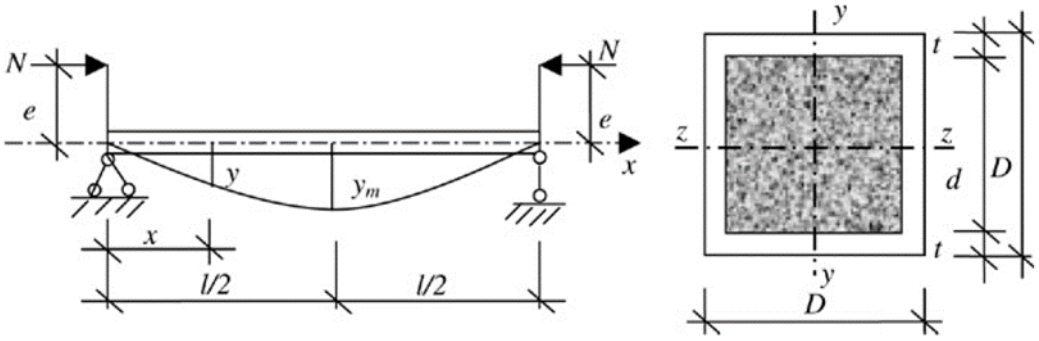

Figure 2.6 The eccentrically compressed square CFST column (Lu et al. 2007).

An investigation study was done by Lam and Gardner (2008) on the compressive behavior of concrete-filled stainless steel columns, with various concrete strength. A comparison was done between compressive resistance of column with the stainless steel hollow. Also, comparisons were held with existing design rules provided by EC4-2004. According to the continuous strength method, a new design formula for calculating the strength and contribution of stainless steel was developed. The test

program included two cross-sectional types, a hollow square and a circular hollow sections. Four different sections size were 100x100x5mm square hollow sections, 100 x100x2mm square hollow sections, 114x6mm circular hollow sections and 104x2mm circular hollow sections. Four test of stub column were done out for each size. Three of them were for the filled concrete samples with nominal concrete strengths of 30MPa, 60MPa and 100MPa. Furthermore, there was a test of empty stainless steel tube. Moreover, separate tests were also conducted in order to achieve component material properties. Furthermore, 16 stub column tests (eight square hollows and eight circular hollows) were applied on the samples having a height of 300 mm, capping thin layer of plaster clamps were used at each end of the sample. One horizontally and two vertically allied strain measures were attached with all columns stub at a height intermediate. Also, the two linear variable deformation transducers existed placed on any lateral of the columns stub for measuring end shorten. It was concluded that the current design guidance in the codes can be safely used for concrete filled stainless steel tubes, in spite of being desperately conservative mainly for circular hollow sections. In addition, the established continuous strength method provided consistent and accurate predictions of the investigation capacity for assessment of the contribution to composite resistance of stainless steel tube.

A study done by Kuranovas et al. (2009) a detailed analysis of the experimental data was presented for more than 1300 specimens of CFST and it covered different types, including hollow and solid concrete core of circular and rectangular cross-section area by applying both concentric and eccentric axial loads with sustained and preloading load. To find the accuracy of the predicted value compared with the actual one, the capacity of the CFST sample was calculated using the approach proposed by EC4-2004. The CFST design requirement 10 proposed in EC4-2004 was concluded to be a good approach to determine the strength of all kinds of circular CFST column studs, showing that the concrete filling strength is smaller than 100 MPa.

An experimental study has been done by Abdalla (2012) presented an experimental study to investigate the influence of the main influencing factors on the compression behavior of a circular CFST columns. The important parameters are compressive strength of concrete, the ratio of diameter-thickness (D/t) and the loading rates. In the test two compressive strengths of 44MPa and 60MPa were applied, D/t ratios of 54,

32, and 20 were used also low loading rates of 0.6 and 60 KN/sec were applied. A nonlinear finite element numerical model was also created and verified by using the suggested experimental results. Also D/t ratio effectiveness on the compressive behavior of the CFST column was found to be more than the impacts of the other factors. Furthermore, the stiffness of the CFST specimens' was strongly affected by the D/t ratio when comparing it to the impact of the concrete infill compressive strength or the loading rate.

Liew et al. (2012) carried a test program to investigate the performance of 27 samples of axial load column, with 18 steel tubes filled of compressive strength equal to 200 MPa of the ultra-high strength concrete, four steel tubes filled with normal concrete strength and five hollow tubes. Into the ultra-high strength concrete the steel fibers were added, to study their influence in attractive the strength and ductility. Concrete filled double-tube columns were also investigated for potential applications in high-rise and multi-story constructions. As shown in the test results that ultra-high strength concrete filled tubular columns realized ultra-high force-carrying capacities but they could become brittle when of the maximum compression was achieved. In addition, the strength and the ductility of composite columns filled with the ultra-high strength concrete was developed by applying load only on the concrete core, addition the steel fibers into the concrete core or increasing contribution of the steel ratio. The test results comparison with the prediction EC4-2004 displays the EC4-2004 method can be safely protracted to predict the resistance compression of the ultra-high concrete strength filled composite stub columns. On average, EC4-2004 approach underestimated the resistance by 14.6% if the confinement influence was not reserved into reason, and 3.5% if the confinement effect was taken into account for all the specimens including ultra-high strength concrete. However, to ensure adequate ductility, it is recommended to use a minimum contribution steel ratio of 0.30 or 1% steel fibers should be used. Furthermore, when estimating the final ultimate load of the concrete filled composite columns with Class 3 steel parts, the improvement in strength because of the confinement influence should be ignored.

2.1.5 Section shapes

Tomii et al. (1977) examined the nearly of 270 circulars, square and octagonal composite columns. The value of D/t was in the range of 19 to 75, and L/D was in

the range of 2 to 9. The result is that the vertical load post-yield behavior (1) strain hardening, (2) perfect plastic; (3) stiffness is reduced. Type 1 or 2 were classified as which one octagonal and circular shapes, while some of the octagonal cross sections and all of the square were categorized as Type 3. At high axial loading, concrete confinement was detected in many octagonal and circular cross sections and the strain hardening properties of these samples were explained.

Schneider (1998) presented analytical and experimental studies on short and CFST columns behavior which were subjected to concentrically loaded until failure compression. 14 specimens were tested to investigate the effect of the steel tube shape and wall thickness on the ultimate strength of the composite column. Confinement of the concrete core provided by the tube shape was also addressed. Depth-tube wall thickness ratios between $17 < D/t < 50$, and the length tube-depth ratios of $4 < L/D < 5$ were investigated. The supervise the design of steel tube columns filled with concrete comparing the result of ultimate strength to the code specifications. A nonlinear finite element model was verified and developed by using the test results. Further also used an analytical model to investigate the validity of the design specification. Experimental results propose that the circular tubes provide substantial stiffness and yield strength and are not available in rectangular or square cross sections. From these results, also found that the design specification is sufficient to predict the yield load under most conditions of various structural shapes.

Chen and Lin (2006) developed an analytical model for anticipating the force-deformation response. Three different shapes of the structural steel section were used; I, H, T cross-shaped sections. The analytical model took into account the relationships between the variables of the materials used such as structural steel section, confined and unconfined concrete, and longitudinal reinforcement bars. In their analytical model, they evaluated the confinement factor for confined areas and they concluded that the steel shapes, the diameter and spacing of the lateral and longitudinal reinforcement, as well as layout of section effect the confining stress which have high pronounced enhancement in the ultimate strength and axial capacity.

2.2 CFST beams (Pure Bending)

Fanning and Kelly (2001) announced the results of the bending test of 10 RC beam reinforced with various plate configurations. In combination with the heuristics obtained from the test data, the strain force and compatibility equilibrium analysis method predicts the final response of a simply supported beam, regardless of the length of the plate, without or with an endplate anchor. It has been shown to be effective. The results observed that the external coupling of the carbon fiber reinforced polymer plate provides a very effective means of reinforcing the reinforce concrete beam in bending. Bending tests carried out in the test program showed that the corresponding anchor plate stiffness increased by 40% and the corresponding anchor plate final strength increased by 70%. As the length of the plate decreases, the effectiveness of the external plate in strengthening decreases.

Elchalakani et al. (2001) showed a bending behavior of a circular CFST subjected to a large deformation was studied by performing a pure bending of D/t 12 to 110. Compare the behaviors of air-filled, empty circular hollow cross-sections cold-formed under purely plastic bending. Concrete filling was found to completely prevent local buckling and elliptification of cold-formed steel tubes with $13 < D/t < 40$, but the in elastic range of CFST of $74 < D/t < 110$, Plastic ripple was detected. Energy absorption, ductility and strengthening are thinner, especially in the case of circular hollow sections. A plasticity limit of D/t 112 was obtained for CFST constructed under pure bending from a cold-formed hollow.

A study done by Han (2004) a mechanics model that can predict the behavior of hollow structural section beams filled with concrete were investigated. A rectangular and square tube beam tests filled with a series of concrete were performed. The main parameters used in the test were varied, a depth-width (D/B) varied from 1 to 2 and tube depth-wall thickness (D/t) varied from 20 to 50. The resulted curves of the load mid-span deflection showed similar results with the presented test results.

Han et al. (2006) investigated a further study on the bending behavior of concrete-filled steel tubes based on previous research. Bending behavior of CFST. Around 36 composite beams sample test filled with Self-Consolidating Concrete (SCC) were tested. Mainly the parameters changed in the test are as follows:

(1) Section type.

(2) Yield strength of steel (235 to 282 MPa).

(3) The ratio of tube diameter (or width) to wall thickness, D/t (47 to 105).

(4) Ratio of shear span to depth (1.25-6).

A comparison is made with the beam capacity predicted using the existing method. The method proposed are used to compare the bending stiffness of the predicted beam. This is a simplified model and generally good results were achieved.

Arivalagan and Kandasamy (2010) presented on the bending and cyclic behavior of CFST beam. The test samples filled by normal concrete mixed, fly ash, low strength concrete and quarry waste concrete and HSS were tested. The deflections and strains measurements were prepared below 4-point loading. The numerically model for predicting moment carrying capacity was also developed. The ultimate capacity had been compared with the beams capacities achieved by using the standards code as follows EC4-1994 and AISC-1999. Experimental investigations have shown that the moment carrying capacity increases based on the compressive strength of the filler material. Because of the energy absorption capacity also increase due to in filled materials. The results analytical show well agreements with the results of experimental. Revealed the results that it there is an increase of 28%, 27% and 25% in the moment carrying capacity of normal concrete mixed, the quarry waste concrete and fly ash, respectively, as compared with the HSS. The theoretical expression developed for the calculation of resistance moment based on Indian code stress block closely predicts the bending behavior. The existing international code formulae (without safety factor) underestimates of moment carrying of the CFST beams. Concrete filling increases the enduring load capacity of the thin square hollow sections and rectangular hollow section beams, especially to resist the cyclic load while the transverse deformation increases. The concrete filling increases the energy absorption especially for HSS.

Xiamuxi and Hasegawa (2011) presented the effect of internal reinforcement in CFST was investigated and it was concluded that the moment capacity, toughness, ductility and seismic performance of RCFST members increased with those of CFST. In other

words, since the operation of RCFST is different from the operation of CFST for internal reinforcement, the evaluation method of CFST operation cannot be applied perfectly to RCFST.

Another study was examined by Guler et al. (2012) the studied the bending behavior of square HSS beam. The test was conducted for six unfilled and nine ultra-high performance concrete-filled HSS beams under four point bending until it reach failure level. The influence of the steel tube thickness, the strength of concrete and the yield strength of the steel tube on moment capacity, curvature and ductility of ultra-high performance concrete-filled HSS beams were tested. The calculated bending strengths were compared with the values determined by AISC360-10 and EC4-2004 design codes. The results revealed that when increasing the thickness of wall thickness of the steel tube, the corresponding curvature and the ultimate moment capacity will be increased for both the hollow and ultra-high performance concrete-filled HSS beams. However, in the case of HSS beams, the thinner beams will achieve more moment capacity and corresponding curvature than the thicker beams. Its noticed that when the steel tube thickness of the HSS beams is reduced from 4 mm to 2.5 mm, there will be a significant increase in the values of relative ductility index and strength increasing factor. The significant increase in both moment capacity and the corresponding curvature is mainly due to the fact that the thinner sections are more vulnerable to local buckling when compared to thicker sections.

Jiang et al. (2013) presented of the four samples of two rectangular samples and two square samples were presented with a ratio of width-thickness (B/t) between (50-100). A curve of displacement load, mode failure and final volume of the samples will be achieved. Developed an analytical model of bending thin walled CFST. In the developed model, the properties of the material limited concrete, a strengthening of the corner strength of the cold-formed steel section, the remaining stress, and local buckling of the plate had taken into account. The suggested model was able to calculate specimen the intensity and behavior of the specimen by reasonable precision. Furthermore, the fitness of the model to the EC4-2004 and AISC360-10 standard bent thin-wall CFST was also evaluated.

Vijay and Manoj (2014) presented a study on the bending behavior of CFST based on the previous efforts shown in Figure 2.7. An ANSYS software model was developed

that can predict the behavior of CFST to determine the moment carrying capacity at the ultimate point. The CFST beam is verified and verified against the experimental data by the finite element method software ANSYS. The main parameters that influence the behavior and strength of concrete filled beams, geometric parameters, load, material nonlinearity, and the boundary conditions. To account for all these characteristics, the ANSYS software model has been developed. The main parameter that changes in analytical research is the D/t ratio, which is the characteristic strength of filled concrete. The proposed model foresees the ultimate moment capacity of the CFST beam. For numerical analysis, rectangular and circular CFST cross sections are taken into account using different grades of concrete. Compare the predicted values with the experiment results. Numerical analysis shows that a good confinement effect can be obtained with a rectangular CFST.

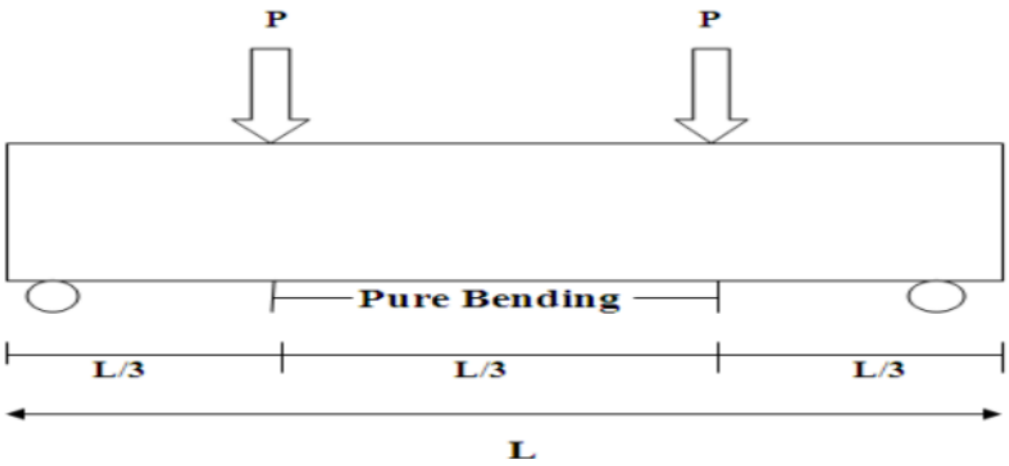

Figure 2.7 Flexure test on CFST beam (Vijay and Manoj, 2014).

Wang et al. (2014) conducted a study where they presented a finite element analysis model, this is to study the bending performance of RCFST members with a compact, non-compact or slender element sections. Validate finite element analysis modeling using 70 test results. Generally, good agreement was obtained in the intermediate member bending capacity and moment curve tendency between the experimental result and the finite element analysis result and the deflection relationship of the intermediate member. The finite element analysis modeling is then used to test the residual failure pattern of the core concrete, the typical residual deformation of the external steel tube, and the strain and stress distribution over the composite section in a full load procedure. The results showed when an interactions happen between concrete and steel

composite beam, it gives stress redistribution to concrete and steel and RCFST beam has high bending capacity and ductility. Finally, the reliability analysis method is used to calibrate existing design formulas of composite beams of EC4-2004, AISC360-10 and technical specification for concrete-filled steel tubular structures in Chinese DBJ/T13-51-2010. It was found that all design formulas achieve appropriate reliability index.

An experimental study done by Ghannam (2016) the investigate bending behavior of a square CFST. As shown in Figure 2.8 where the depth-thickness ratio (D/t) are 23.8 and 27.8. A comparison was made between the behavior of both hollow hot rolling section of concrete filling material and the empty hot rolling section by under pure bending. The behavior of CFST beam partially replaced by coarse aggregate using granite under bending load is shown. Effect of steel tube, confinement of concrete and compressive strength of concrete were investigated. six samples were tested at concrete strength of 20 MPa. The beams dimensions are 88.9x88.9mm, 114.3x114.3 mm, and the length is 1200 mm. The results of the test, showed that the final load holding capacity of the steel tube beam in which the coarse aggregate was partially replaced by granite was almost the same as that of concrete maintenance material. In general, filled steel tubes increase ductility, strength and energy absorption, especially for thin parts. The steel shell results in the constraint of the concrete core, and improved core strength and ductility.

Figure 2.8 Test set up (Ghanname, 2016).

2.3 Combined Axial Load and Bending Moment on CFST beam-columns

As shown in Figure 2.9, the ultimate strength of the members subjected to a combined axial load and bending moment capacity (beam-columns) is often described as a *P-M* interaction curve. M_0 in the Figure 2.9 represents the pure bending moment capacity when no axial load is applied. In the case of steel members, M_0 coincides with the maximum moment capacity, while the curve for the concrete member's bulges at a certain level of the axial load with the maximum moment exceeding M_0, with some amount of axial loads applied, the larger portion of the concrete in the section is under compression, contributing to the moment strength of the member (concrete with tension has generally negligible effects). It is generally accepted that the interaction curve for CFST members is similar to that for concrete, since there is concrete in the section.

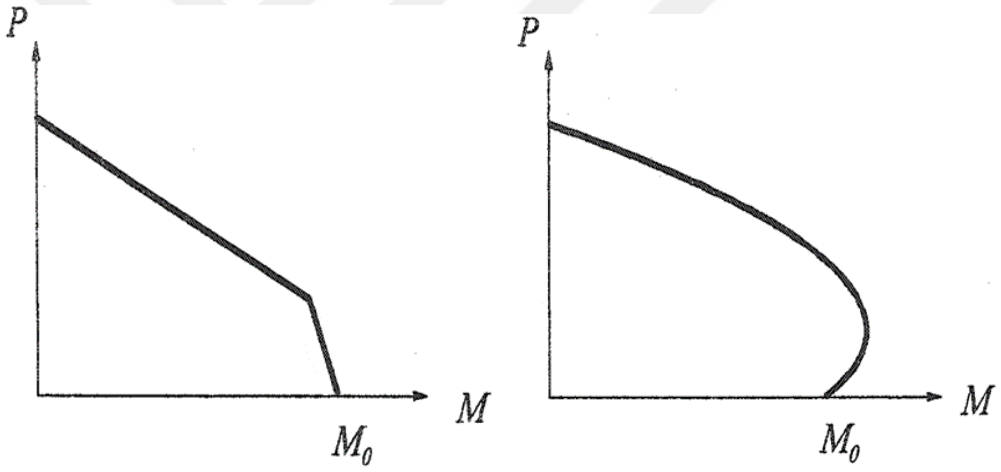

Steel structures RC structures

Figure 2.9 Typical P-M Interaction Curve (AISC360-10).

Schiller et al. (1994) summarized the recommended value of elastic stiffness for RCFST with a focus on the use in nonlinear beam-columns element formulations. The axial, bending, shear, and torsional stiffness, were investigated separately making comparisons with the available experimental results. It was determined that for axial and bending elastic stiffness, using the total gross sectional properties and initial stiffness were appropriate for the purpose of the elastic component of the concentrated plasticity element. However, an alternative bending stiffness was recommended for

more general use within elastic analysis in which only a portion of the bending stiffness from the concrete is included.

Kawaguchi et al. (1998) compiled an experimental database for CFST beam-columns from tests conducted in Japan. The collected data included monotonic and cyclic loads and documented material and geometric properties, experimental stiffness, and strengths and deformations associated to the peak and other characteristic levels (i.e. post-peak strength dropped 5%, maximum rotation reached the 1/100 value). Based on the experimental data, these authors developed an analytical model for the calculation of the bending strength and the rotational capacity of CFST beam-columns.

Gourley et al. (2001) noted that width-thickness (B/t), axial load ratio, and slenderness of the member were the most important factors among others for beam-column behavior of CFST members. B/t was thought to be the most important factor, as it determined the point of local buckling. The axial load ratio was thought to be the second, and slenderness of the member follows in importance. The point of local buckling is delayed for CFST members with a small B/t. When the applied axial loads are approximately 50% of squash load, the CFST members show a weak behavior and loses their capacity rapidly.

Han et al. (2004) presented a mechanical model for circular hollow section beam-columns of steel filled with concrete has been developed. A unified theory in which a confinement coefficient (ξ) is introduced to describe the combined action of steel tube and filled concrete is described. The predicted load vs deformation relationship is in good agreement with the test results. The theoretical model was used to investigate the influence of important parameters determining the final strength of concrete-filled steel circular hollow section beam-columns. Parametric and experimental studies provide information for the development of equations for calculation of the final intensity of a composite beam-columns. Compare the expected beam-column intensities using existing codes such as EC4-1994, AISC355-1999, Architectural Institute of Japan (AIJ-1997), and British Standard (BS5400-1979). A basic model has been developed to calculate the cross-sectional volume, member capacity and moment capacity of concrete-filled steel circular hollow section members. Simplified interaction curves are derived for steel circular hollow section beam-columns filled with concrete. Comparisons are also made with column strength predicted using EC4-

1994, AISC355-1999, AIJ-1997, and BS5400-1979. The code is generally conservative (about 10% to 25%). The ability predicted by the simplified model is about 4% to 10% lower than the capability obtained in the test.

Choi et al. (2006) presented a new method to design CFST beam-columns based on the AISC360-05, which is known to provide an over-conservative estimation of strength. The over-conservativeness of the AISC360-05 method comes mainly from ignoring the contribution of the concrete in flexure and the different behavior of composite beam-columns from pure steel beam-columns. The new method reported here assumes full composite action and idealizes the *P-M* interaction curve with two lines, as in the AISC360-05 method. However, the lines intersect at the point where a maximum moment occurs. A complete parametric study is performed using fiber analysis to determine the maximum moment (normalized with nominal moment strength) and the axial load ratio at the maximum moment with respect to tube width-thickness ratio (B/t) and relative concrete compressive strength-yield strength of the steel tube (f_c'/f_y). The strengths based on the modified AISC360-05 *P-M* interaction equations for square CFST columns subjected to axial load and single axis bending moment capacities are compared with a wide range of experimental data, and they show greatly improved results when compared to the AISC360-05 design equations.

Roeder et al. (2010) presented a study which addresses to a combination of axial load and bending moments capacities. In order to determine the best models for predicting the resistance and stiffness of circular CFST. A database of 122 samples was compiled and evaluated. This result shows that the plastic stress method is a simple, but effective way to predict the resistance of a circular CFST components under combined loading. These data indicate that the current specifications provide inaccurate predictions of the bending stiffness and a new stiffness expression is proposed. The proposed models permit for simple yet accurate predictions of resistance and stiffness, allow engineers to routinely use CFST components in structural design.

In a study done by Uy et al. (2011) a couple of tests were undertaken on both slender and short filled concrete, this is to find out their performance under an axial force. Also, for the reason of comparison, the short steel blank hollow sections were also tested. According to the obtained results, the performance of composite columns was greatly good and its accepted to be used in structural members widely. Morever, these

results were also compared with some existing designs of conventional filled concrete based on various codes including AISC360-05, EC4-2004, and Australian Standard (AS 5100-2004). The results of the comparison showed that all the mentoned codes are partially conservative in calculating the load capacity of both short column and slender columns.

Perea and Leon (2011) discussed the results obtained from nonlinear fiber element analysis of CFST. These studies were aimed primarily to evaluate the overall behavior and stability impact of these structural elements as a prelude to a large-scale full-scale test program. Focuses on the final strength analysis of CFST composite columns using different stress-strain models for both steel and concrete. Fiber analysis using open sees evaluates the effect on the final strength based on both the stress-strain curve assumed, the material fineness, the initial imperfections, and both material and geometric nonlinearity. It is used for. Fiber analysis results are also compared with those obtained from AISC360-05. Fiber based results show a compatible correlation with the expected behavior of the elements and are also incorporated into the AISC360-05 specifications.

Zubydan and ElSabbagh (2011) developed a mathematical model was developed to evaluate the monotonic and cyclic behavior of a CFST beam-columns with a rectangular cross section. This model involves a reduction in the compressive strength of the steel due to the local buckling effect. It includes the reloading stiffness of steel tube due to local buckling. In the model, the uniaxial stress-strain material law is used for cross-sectional parts. The results obtained from the mathematical model were compared with the experimental results of the columns under monotonic and cyclic loading. It was found that neglecting local buckling effect may overestimate the maximum and/or the post-peak capacity according to the tube geometry and the material properties. On the other hand, the results obtained from the present model gave good convergence with the experimental results for cross sections as well as columns under monotonic and cyclic loading.

Lai (2014) presented the evaluation and development of these design rules were shown. CFST members reviewed the available experimental databases and created a new experimental database of tests performed on non-compact and thin CFST members. A detailed 3D finite element method model was developed for compact, thin

and long CFST members and benchmarked using experimental results. The compact and thin CFST member AISC360-10 design rules are evaluated by experimental test results and additional finite element method analysis that deals with experimental database gaps. The AISC360-10 axis load and bending moment capacities *P-M* interaction equation has been updated using the results of a comprehensive parametric study (indicated using a benchmarked finite element method model). Effective stress-strain curves of steel tubes and concrete fillers are also progressing. Validation of these effective stress-strain curves was confirmed by implementing them in a macro model based on benchmarked nonlinear fiber analysis.

Lai and Griffis (2015) presented evaluate the applicability of the developed design equations: (i) Compact CFST beam- columns design, and (ii) Estimate the available strength of CFST members within a frames designed using direct analytical methods. The applicability to the design a compact CFST beam-column is evaluated by comparing the resulting *P-M* interaction curves from the developed equation, the equation calculated using the plastic stress dispersion method specified by AISC360-10. The applicability for the direct analysis method is evaluated by comparing the available strengths estimated using the developed equations with demands calculated by conducting second-order elastic analysis using MASTAN2 software. The tube slenderness ratio (λ), material strength ratio (f_y/f_c'), axial load ratio (α) and member length-depth ratio (L/B or L/D). The authors presented a numerical result of evaluating the influence of these four parameters and developed a *P-M* interaction equation to design a non - compact and thin CFST beam-columns.

CHAPTER 3

DESIGN CONCEPT

3.1 General

In this chapter, the design of composite steel and concrete of RCFST structure members explained by AISC360-10 and EC4-2004. These codes are used in the calculation of Chapter 4 on bending moment and axial load capacities of RCFST members.

As shown in Figure 3.1, the notation of geometric dimensions and summarizes the formulas for calculating the geometrical properties (height of rectangular (H), width of rectangular (B), thickness of the steel tube (t), clear distance longer side (h_i), clear distance shorter side (b_i), external radius of steel (r_s), internal radius of concrete (r_c), area of concrete fill (A_c), area of steel tube (A_s), plastic section modulus of concrete (Z_c), plastic section modulus of steel (Z_s), moment of inertia of the concrete (I_c), moment of inertia of the steel tube (I_s)) of concrete and steel materials in Table 3.1. For the HSS, the geometrical properties of the steel tube can also be obtained from the AISC360-10 and EC4-2004 manuals. Since the equation in Table 3.1 does not consider the radius of the fillet, there is a small difference with respect to the moment of inertia of steel tube and the plastic section modulus.

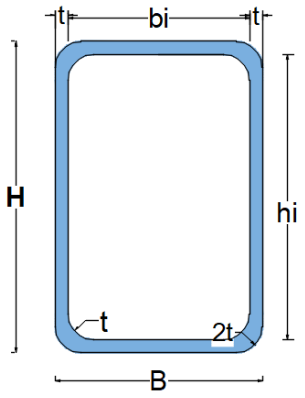

Figure 3.1 Notation in geometric dimensions for RCFST

Table 3.1 Geometric properties for RCFST

Concrete filled tube	Steel tube
$h_i = H - 2t \qquad b_i = B - 2t$ $r_c = r_s - t = t$	$r_s \approx 2t$
$A_c = b_i h_i - (4 - \pi) r_c^2$	$A_s = BH - (4 - \pi) r_s^2 - A_c$
$Z_s = \frac{bh^2}{4} - Z_c$	$Z_c = \frac{b_c h_c^2}{4}$
$I_c = \frac{b_i h_i^3}{12}$	$I_s = \frac{BH^3}{12} - I_c$

3.2 Design Steps of AISC360-10 Code for Capacity Calculation

The design of composite members in AISC360-10 has two methods the plastic stress distribution method and the strain compatibility method. The plastic stress distribution method is the most common method, which provides a simple calculation for the most design situations while the strain compatibility method provides a general calculation method. The plastic stress distribution method used to determine the composite sections nominal strength. However, for special cases such as when the cross-sectional area changes the strain compatibility method would be better choice.

3.2.1 Nominal strength of composite sections

By using AISC360-10, there are two methods to calculate the nominal strength of the composite section. The first one is plastic stress distribution method and the second one is strain compatibility method. When determining a nominal strength of a composite part, the tensile strength of the concrete should be ignored. In this study, the plastic stress distribution method was applied.

3.2.1.1 The method of plastic stress distribution

In the plastic stress distribution method, in the case of a rectangular HSS in which the steel material reaches a yield stress of (f_y) under each compression or tension and the concrete constituent of axial and/or compression because of the deflection is filled with $0.85f_c'$ concrete. In the case of circular HSS filled with concrete, it is permitted to use a stress of $0.95\ f_c'$ for concrete parts with even compression to calculate the influence of the concrete containment.

According to the mentioned assumptions, the cross-section strengths of diverse arrangements of bending moment and axial load capacities are typical Figure 3.2 is the cross-sectional shapes assessment of the composite compression member. As shown in Figure 3.2, based on plastic stress distribution, the interaction diagram of bending moment and axial load capacities of composite part is similar to the reinforced concrete part. As a simplification, specifically enclosed sections can use a discreet linear interaction between 4 or 5 anchor points, subject on the alignment of flexible. These points are defined as A, B, C, D and E in Figure 3.2.

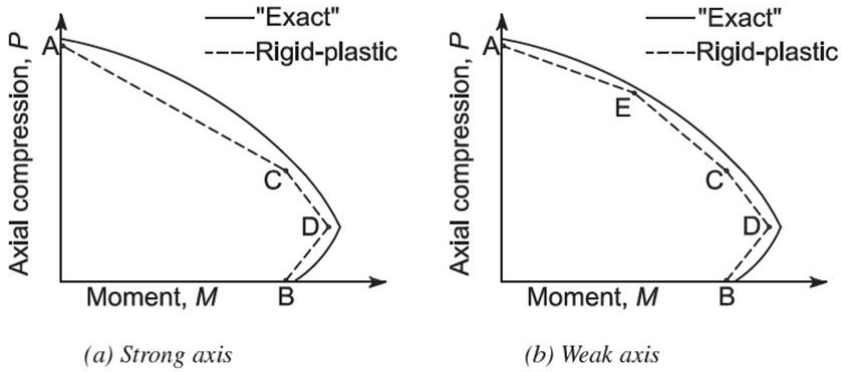

Figure 3.2 Actual interaction between moment and axial force (AISC360-10).

3.2.1.2 Strain compatibility method

In the case of the strain compatibility method, a straight line distribution of the strain through the section. Assume that the maximum concrete compressive strain is equal to 0.003 (mm/mm). The stress-strain relationship of steel and concrete was obtained in published tests results or similar materials.

3.2.2 Material limitations for AISC360-10

Concrete and steel reinforcing bars in composite systems shall be subject to the following limitations:

- Concrete compressive strength (f_c') should be between 21 *MPa* and 70 *MPa*, this is for the case of normal weight concrete and between 21 *MPa* and 42 *MPa* for the case of lightweight concrete.
- For the structural steel and reinforcement bars the minimum yield stress (f_y) should not exceed 525 *MPa*.

3.2.3 Filled composite sections classification for local buckling

In the case of compression, the filled composite sections are classified as compact, non-compact or slender. For a section to qualify as compact, the maximum width-thickness ratio (B/t) of its compression steel elements shall not exceed the limiting B/t, λ_p, from Table 3.2. If the maximum B/t of one or more steel compression elements exceeds λ_p, but does not exceed λ_r from Table 3.2, the filled composite section is non-compact. If the maximum B/t of any compression steel element exceeds λ_r, the section is slender. The maximum allowable B/t shall be as specified in the Table 3.2.

Table 3.2 Limiting width-thickness ratios for compression steel elements in composite members subject to axial compression.

Description of Element	Width-to-Thickness Ratio	λ_p Compact/ Noncompact	λ_r Noncompact/ Slender	Maximum Permitted
Walls of Rectangular HSS and Boxes of Uniform Thickness	b/t	$2.26\sqrt{\frac{E}{F_y}}$	$3.00\sqrt{\frac{E}{F_y}}$	$5.00\sqrt{\frac{E}{F_y}}$
Round HSS	D/t	$\frac{0.15E}{F_y}$	$\frac{0.19E}{F_y}$	$\frac{0.31E}{F_y}$

In the case of flexure, the filled composite parts are classified as compact, non-compact or slender. For compartments deemed to be compact, the maximum B/t of the compressed steel element shall not exceed the limiting B/t λ_p in Table 3.3. If the maximum B/t of one or more steel compression elements exceeds λ_p, but not exceeding λ_r from Table 3.3, that section is non-compact. If the B/t of any steel element exceeds λ_r, the section is slender. The maximum ratio between of allowable B/t is as shown in the Table 3.3.

Table 3.3 Limiting width-thickness ratios for compression steel elements in composite members subject to flexure.

Description of Element	Width-to-Thickness Ratio	λ_p Compact/ Noncompact	λ_r Noncompact/ Slender	Maximum Permitted
Flanges of Rectangular HSS and Boxes of Uniform Thickness	b/t	$2.26\sqrt{\frac{E}{F_y}}$	$3.00\sqrt{\frac{E}{F_y}}$	$5.00\sqrt{\frac{E}{F_y}}$
Webs of Rectangular HSS and Boxes of Uniform Thickness	h/t	$3.00\sqrt{\frac{E}{F_y}}$	$5.70\sqrt{\frac{E}{F_y}}$	$5.70\sqrt{\frac{E}{F_y}}$
Round HSS	D/t	$\frac{0.09E}{F_y}$	$\frac{0.31E}{F_y}$	$\frac{0.31E}{F_y}$

3.2.4 Axial load (columns)

The design compressive strength $\emptyset_c P_n$, and permissible compressive strength, P_n/Ω_c, for axial load filled composite columns shall be determined for the limiting state of bending buckling based on member slenderness as follows:

The AISC360-10 code specification for determining the ultimate load (P_n) of a RCFST column is given by Eqs. (3.1) and (3.2).

Load Resistance Factor Design (LRFD) $\phi_c = 0.75$ and Allowable Stress Design (ASD) $\Omega_c = 2.00$

(a) When $\frac{P_{no}}{P_e} \leq 2.25$ $\quad P_n = P_{no}\left[0.658^{\frac{Pno}{Pe}}\right]$ (3.1)

(b) When $\frac{P_{no}}{\mathrm{Pe}} > 2.25$ $\quad P_n = 0.877P_e$ (3.2)

Where the P_{no} is nominal compressive strength of zero length (N), P_n is nominal axial strength (N), and the (P_e) is elastic critical buckling load (N) can be calculated according to Euler's formula, of the AISC360-10 code as shown in Eq. (3.3).

$$P_e = \frac{\pi^2(EI_{eff})}{(kL)^2} \tag{3.3}$$

Where k is the effective length factor and it is as shown in Table 3.4 and L is the laterally unbraced length of the member (mm).

Table 3.4 Approximate Values of Effective Length Factor, K

Buckled shape of column shown by dashed line	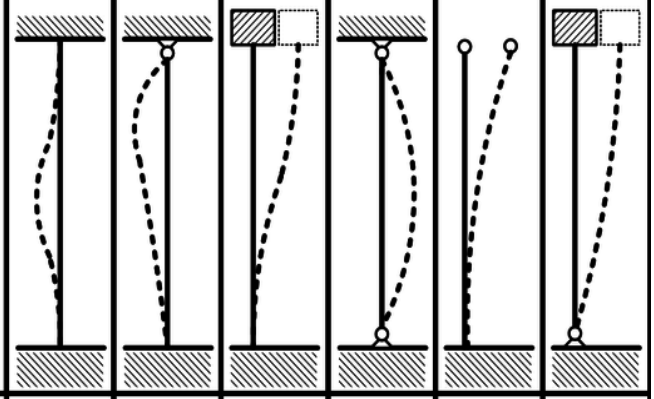					
Theoretical K value	0.5	0.7	1.0	1.0	2.0	2.0
Recommended design value K	0.65	0.80	1.2	1.0	2.10	2.0
End condition key		Rotation fixed and translation fixed Rotation free and translation fixed Rotation fixed and translation free Rotation free and translation free				

EI_{eff} is effective stiffness of composite section ($N.mm^2$) is determined from Eq.(3.4)

$$EI_{eff} = E_s I_s + C_1 E_c I_c \tag{3.4}$$

Where E_s is modulus of elasticity of steel (200000 MPa), I_s is moment of inertia of the steel (mm^4), E_c is modulus of elasticity of concrete ($0.043 w_c^{1.5} \sqrt{f_c'}$, MPa), w_c is weight of concrete per unit volume ($1500 \leq w_c \leq 2500$, kg/m^3), I_c is moment of inertia of concrete (mm^4) and C_1 is coefficient for calculation of effective rigidity of an encased composite compression member Eq. (3.5).

$$C_1 = 0.1 + 2\left(\frac{A_s}{A_c + A_s}\right) \leq 0.3 \tag{3.5}$$

Where A_s is cross-sectional area of steel section (mm^2) and A_c is cross-sectional area of concrete (mm^2).

Figure 3.3 shows the nominal axial compressive strength of zero length (P_{no}) composite section of HSS slenderness. As shown in Figure 3.3, the compact section complete plastic nominal bearing strength (P_p) can be expressed at the time of compression. Nominal axis direction the intensity P_{no} of the non-compact section can be found using quadratic interpolation between the plastic strength P_p and the axial yield strength (P_y) tube slenderness. This interpolation is secondary.

Capacity of steel tube includes concrete filling subject to inelastic and volume expansion. It decreases rapidly with the HSS. Slender section is limited to development important buckling resistance of steel HSS critical stress (F_{cr}) and $0.70f_c'$ of concrete infill.

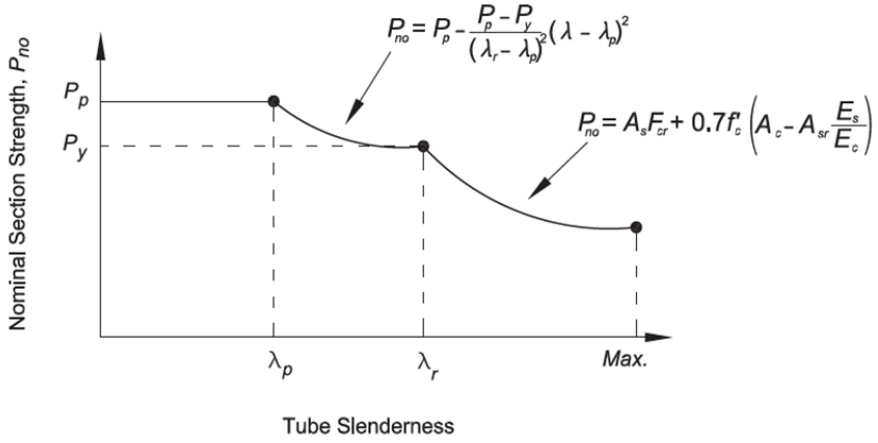

Figure 3.3 Nominal axial strength, P_{no} versus HSS slenderness (B/t) (Lai and Zhang, 2014).

a) Compact Sections

In the case of a compact section ($\lambda \leq \lambda_p$), the nominal compressive strength of zero length (P_{no}) of an axially loaded of RCFST can be determined with respect to the limit state of flexural buckling as shown in Eq. (3.6).

$$P_{no} = P_p = f_y A_s + 0.85\, fc' A_c \tag{3.6}$$

b) Non-Compact Sections

In the case of non-compact section ($\lambda_p \leq \lambda \leq \lambda_r$), the nominal compressive strength of zero length (P_{no}) of an axially loaded of RCFST can be calculated from Eqs. (3.7), (3.8) and (3.9).

$$P_{no} = P_p - \frac{P_p - P_y}{(\lambda - \lambda_p)^2}(\lambda - \lambda_p)^2 \tag{3.7}$$

$$P_p = f_y A_s + 0.85\, fc' A_c \tag{3.8}$$

$$P_y = f_y A_s + 0.7 fc' A_c \tag{3.9}$$

c) Slender Sections

In the case of slender section ($\lambda_r \leq \lambda \leq \lambda_{max}$), the nominal compressive strength of zero length (P_{no}) of an axially loaded of RCFST can be determined from Eq. (3.10).

$$P_{no} = F_{cr} As + 0.7 fc' A_c \tag{3.10}$$

$$F_{cr} = \frac{9\, E_s}{(\frac{b}{t})^2} \tag{3.11}$$

The effective stiffness of the composite section (EI_{eff}) can be calculated for all sections using the following Eq. (3.12).

$$EI_{eff} = E_s I_s + C_3 E_c\, I_c \tag{3.12}$$

Where C_3 is coefficient for calculation of effective rigidity of the filled composite compression member, is determined from Eq. (3.13).

$$C_3 = 0.6 + 2\left(\frac{A_s}{A_c + A_s}\right) \leq 0.9 \tag{3.13}$$

3.2.5 Bending moment capacities (beams)

If ($\lambda \leq \lambda_p$) compact section. The distance of the neutral axis (a_p) from the compression face is calculated by establishing axial force equilibrium over the cross-section, the plastic moment strength (M_p), and the nominal flexural strength (M_n). The

Eqs. (3.14) and (3.15) for calculating a_p and $M_p$are used. The variables of these equations are shown in Figure 3.4. In these equations H, b, t_w, t_f are the tube depth, width, web thickness, and flange thickness respectively.

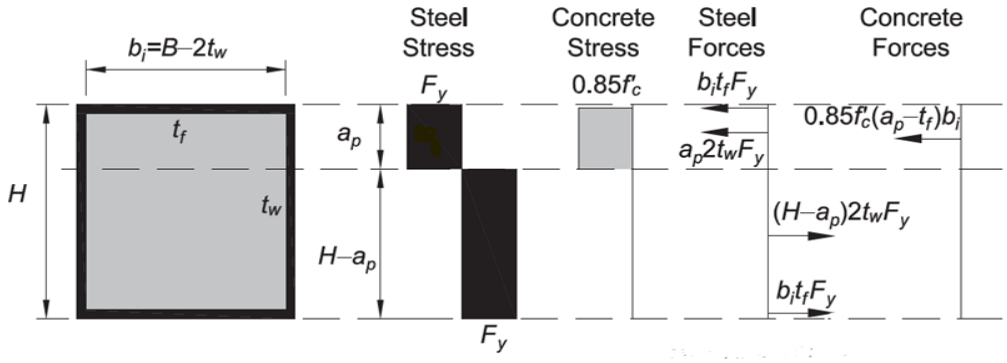

Figure 3.4 Compact section-stress blocks for calculating M_p (Lai and Zhang, 2014).

$$a_p = \frac{2F_y H t_w + 0.85fc' b_i t_f}{4t_w F_y + 0.85fc' b_i} \tag{3.14}$$

$$\begin{aligned} M_n = M_p = {} & F_y b_i t_f \left(a_p - \frac{t_f}{2}\right) + F_y b_i t_f \left(H - a_p - \frac{t_f}{2}\right) + F_y a_p 2t_w \left(\frac{a_p}{2}\right) \\ & + F_y (H - a_p) 2t_w \left(\frac{H - a_p}{2}\right) \\ & + 0.85fc' (a_p - t_f) b \left(\frac{a_p - t_f}{2}\right) \end{aligned} \tag{3.15}$$

Non-compact section ($\lambda_p \leq \lambda \leq \lambda_r$) Figure 3.4. As shown, to estimate the minimum binding capacity of non-compact sections with tube slenderness (λ)= λ_r. The distance of the neutral axis (a_y) from the compression face is calculated by establishing axial force equilibrium over the cross-section, and the moment capacity (M_n= M_y) is calculated using this neutral axis location as shown in Eqs. (3.16) and (3.17) for calculating a_y and M_y are shown in Figure 3.5.

$$a_y = \frac{2F_y H t_w + 0.35fc' b_i t_f}{4t_w F_y + 0.35fc' b_i} \tag{3.16}$$

$$\begin{aligned} M_n = M_y = {} & F_y b_i t_f \left(a_y - \frac{t_f}{2}\right) + F_y b_i t_f \left(H - a_y - \frac{t_f}{2}\right) + 0.5F_y a_y 2t_w \left(\frac{2a_y}{3}\right) \\ & + 0.5F_y a_y 2t_w \left(\frac{2a_y}{3}\right) + F_y (H - 2a_y) 2t_w \left(\frac{H}{2}\right) \\ & + 0.35fc' (a_y - t_f) b \left[\frac{2(a_y - t_f)}{3}\right] \end{aligned} \tag{3.17}$$

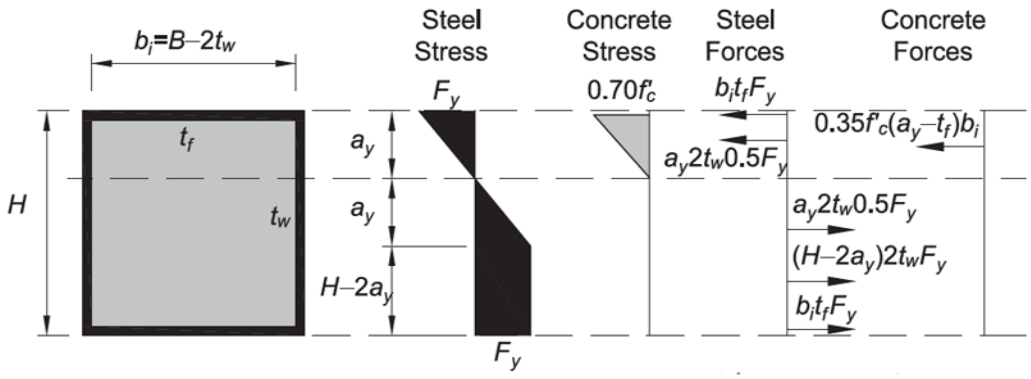

Figure 3.5 Noncom pact section-stress blocks for calculating M_y (Lai and Zhang, 2014).

For an uncompressed section with tube slenderness (λ) is greater than λ_p but less than or equal to λ_r, the nominal moment capacity M_n can be calculated using Eq.(3.18).

$$M_n = M_p - \frac{(M_p - M_y)}{(\lambda_r - \lambda_p)}(\lambda - \lambda_p) \tag{3.18}$$

Figure 3.6 shows the change in nominal bending strength, M_n, of the filling HSS slender section. As illustrated, complete plastic deflection strength, M_p, non-compact nominal bending strength, M_n, sections can be determined using linear interpolation between plastics strength, M_p, moment at yield strength, M_y, HSS slenderness. Slender section are limited to development the first yield moment, M_{cr}, of the composite section the tension flange first contracts and the compression flange. It is limited to the critical buckling strength, F_{cr}, and the concrete is limited to linear elasticity behavior with maximum compressive stress equal to $0.70f_c'$.

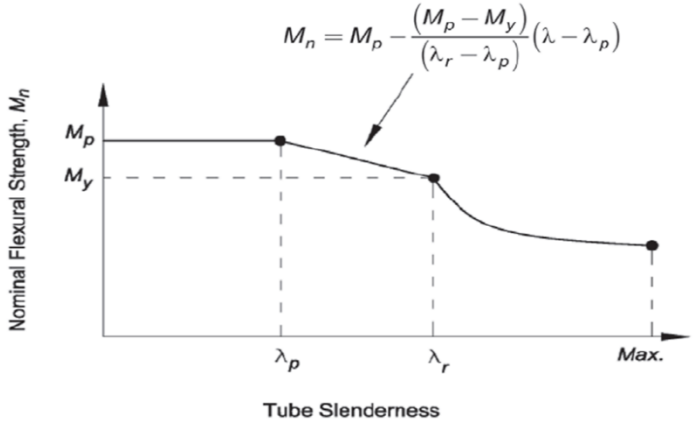

Figure 3.6 Nominal bending moment capacity of filled beam versus HSS slenderness (Lai and Zhang, 2014).

Slender section ($\lambda_r \leq \lambda \leq \lambda_{max}$) evaluate the minimum bending capacity of the slender sections as shown in Figure 3.7. Eqs. (3.19) and (3.20). The distance of the neutral axis (a_{cr}) from the compression face is calculated by establishing axial force equilibrium over the cross-section, and the moment capacity ($M_n = M_{cr}$). The variables of these equations are schematically defined in Figure 3.7.

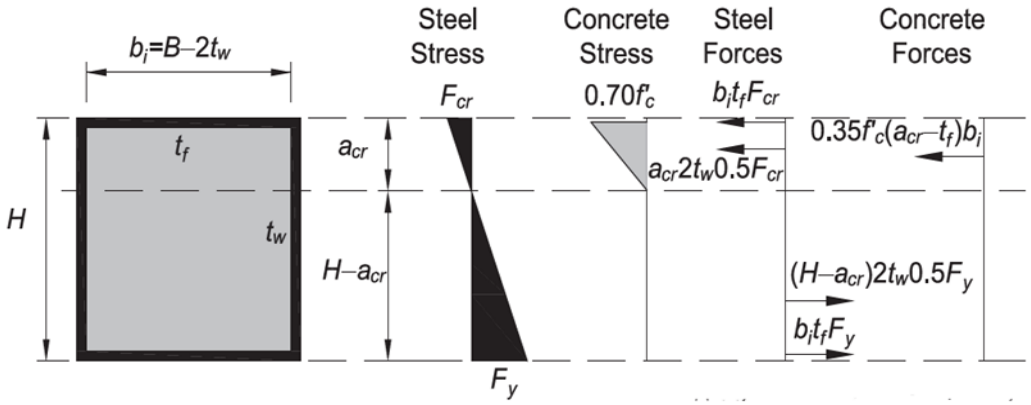

Figure 3.7 Slender section-stress blocks for calculating first yield moment, M_{cr} (Lai and Zhang, 2014).

$$a_{cr} = \frac{F_y H t_w + \left(0.35fc' + F_y - F_{cr}\right) b_i t_f}{t_w(F_{cr} + F_y) + 0.35fc' b_i} \tag{3.19}$$

$$\begin{aligned} M_n = M_{cr} = {} & F_{cr} b_i t_f \left(a_{cr} - \frac{t_f}{2}\right) + F_y b_i t_f \left(H - a_{cr} - \frac{t_f}{2}\right) + 0.5F_{cr} a_{cr} 2t_w \left(\frac{2a_{cr}}{3}\right) \\ & + 0.5F_{cr}(H - a_{cr}) 2t_w \left(\frac{2(H - a_{cr})}{3}\right) \\ & + 0.35fc'\left(a_{cr} - t_f\right) b \left(\frac{2(a_{cr} - t_f)}{3}\right) \end{aligned} \tag{3.20}$$

3.2.6 Combined flexure and axial force (beam-columns)

Interaction curves as shown in Figure3.8 from the plastic stress distribution model are illustrated in Table 3.5 calculated and applied to each points.

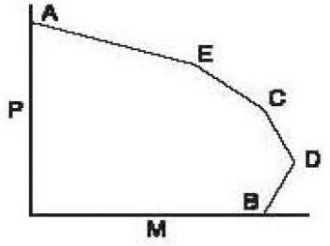

Figure 3.8 Filled rectangular HSS, strong-axis anchor points (AISC360-10)

Table 3.5 Plastic capacities for composite filled HSS bent about either principal axis

Section and Stress Distribution	Pt.	Defining Equations
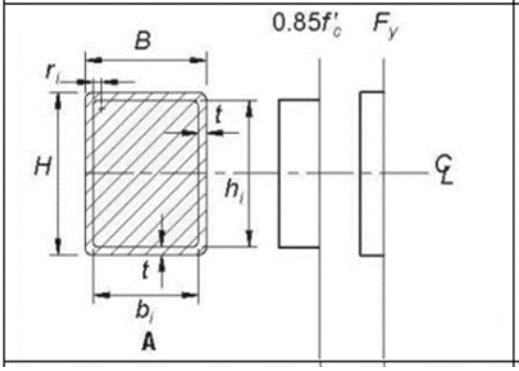	A	$PA = FyAs + 0.85fc'Ac$ $MA = 0$ $As = area\ of\ steel\ shape$ $t = r$ $Ac = bihi - 0.858r^2$ $bi = B - 2t$ $hi = H - 2t$
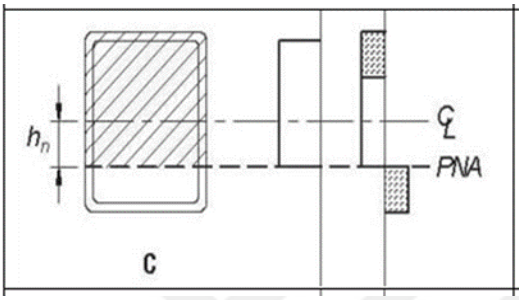	C	$Pc = 0.85fc'Ac$ $Mc = MB$
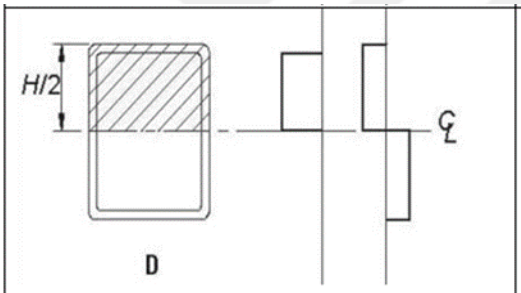	D	$PD = \frac{0.85fc'Ac}{2}$ $MD = FyZs + \frac{0.85fc'Zc}{2}$ Zs $= full\ x$ $- axis\ plastic\ section\ modulus\ of\ HSS$ $Zc = \frac{bihi^2}{4} + 0.192r^2$
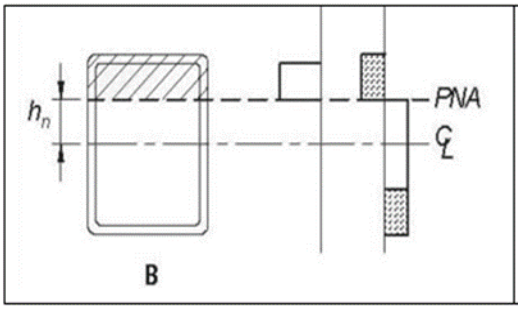	B	$PB = 0$ $MB = MD - FyZsn - \frac{0.85fc'Zcn}{2}$ $Zsn = 2thn^2$ $Zcn = bihn^2$ $hn = \frac{0.85fc'Ac}{2[0.85fc'bi + 4tFy]} \leq \frac{hi}{2}$
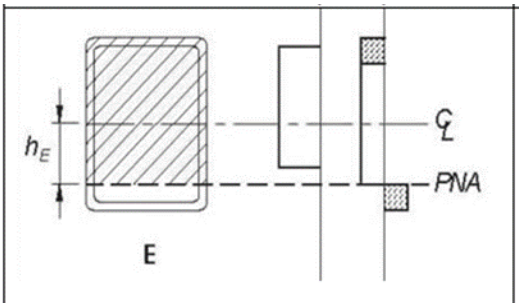	E	$PE = \frac{0.85fc'Ac}{2} + 0.85fc'bihE + 4FythE$ $ME = MD - FyZsE - \frac{0.85fc'ZcE}{2}$ $ZcE = bihE^2$ $ZsE = 2thE^2$ $hE = \frac{hn}{2} + \frac{H}{4}$

3.3 EC4-2004

There are two approaches adopted by the EC4-2004 for calculating the axial load and bending moment capacities of a composite members, the general method and the simplified method. In this study, the simplified method was applied.

3.3.1 Simplified method of design

The simplified method is limited to symmetrical cross-sectional members and a uniform cross-section. When the structural steel component has two or more unconnected parts, the simplified method is not applicable. The imperfections of element implicitly taken into account.

3.3.2 Limitations of EC4-2004

- The axial reinforcement that can be used for calculations shall not over 6% of the concrete area.
- The cross-section depth-width ratio of the composite cross section shall be within the range of 0.2 and 5.0.
- The maximum non-dimensional slenderness ratio of the composite members $\bar{\lambda}$ is limited to 2.0.

Table 3.6 Maximum values (d/t), (h/t) and (b/t_f) with f_y in N/mm^2

Cross-section	max (d/t), max (h/t) and max (b/t)
Circular hollow steel sections 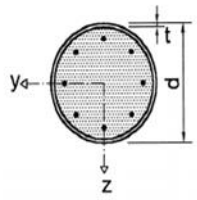	$\max\ (d/t) = 90\dfrac{235}{f_y}$
Rectangular hollow steel sections 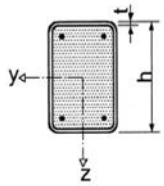	$\max\ (h/t) = 52\sqrt{\dfrac{235}{f_y}}$

3.3.3 Combined compression and bending (beam-columns)

The resistance of a composite member subjected to combined compression and bending is determined from an interaction curve as shown in Figure 3.9.

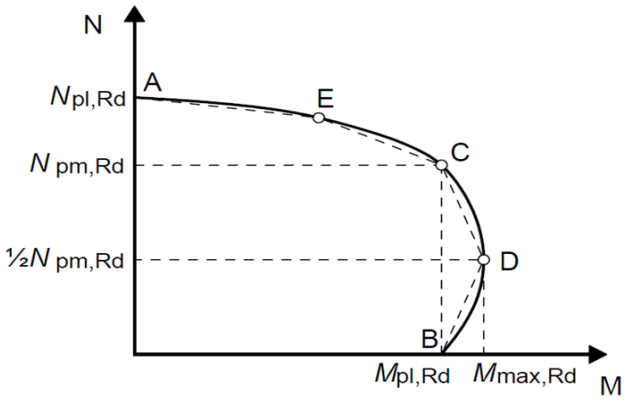

Figure 3.9 Interaction curve and corresponding stress distributions (Twilt et al. 1994)

Point (A) as shown in Figure 3.10, the plastic resistance of the cross-section against compression when no bending moment is applied as shown in Figure 3.10. Calculated the final axial compressive strength of the formula CFST column, compressive normal force ($N_{pI,Rd}$) at Eq. (3.21).

$$N_A = N_{pI,Rd} = A_a f_{yd} + A_c f_{cd} \quad \text{(kN)} \tag{3.21}$$

Where A_a is cross-sectional area of the structural steel section, A_c is cross-sectional area of concrete, f_{yd} is design value of the yield strength of structure steel ($f_{yd} = f_y/\gamma_a$), γ_a is partial safety factor of steel, and f_{cd} is design value of the cylinder compressive strength of concrete ($f_{cd} = f_{ck}/\gamma_c$), γ_c is partial safety factor of concrete.

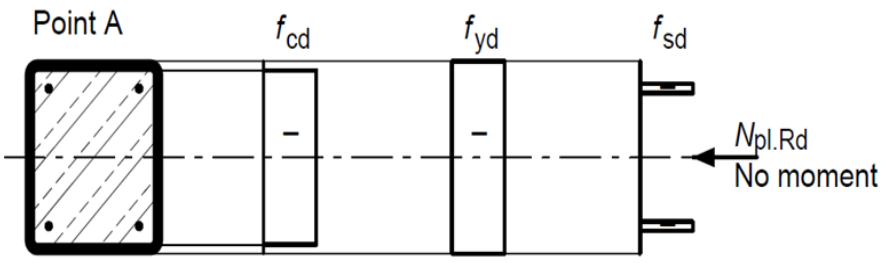

Figure 3.10 Stress distribution with point (A) on the interaction curve of concrete filled hollow cross section at $M_A = 0$ (Twilt et al. 1994).

Point (B) as shown in Figure 3.11, corresponds to the plastic moment resistance of the cross-section can be calculated from Eq. (3.22) when no axial load is applied as shown in Figure 3.11.

$$M_B = M_{pI,Rd} = f_{yd}\left(W_{pa} - W_{pan}\right) + 0.5 f_{cd}\left(W_{pc} - W_{pcn}\right) + f_{sd}\left(W_{ps} - W_{psn}\right) \quad (3.22)$$

Where $M_{pI,Rd}$ is the plastic resistance of moment, W_{pa}, W_{pc},and W_{ps} are the plastic section moduli for the steel section, the concrete of the composite cross-section (assumed to be un-cracked) and the reinforcement respectively. W_{pan}, W_{pcn}, and W_{psn} are the plastic section moduli of the corresponding components within the region of $2h_n$ from the center-line of the composite cross-section.

In the case of rectangular hollow section the W_{pc} can be determined from Eq. (3.23).

$$W_{pc} = \frac{(b-2t)(h-2t)^2}{4} - \frac{2}{3}\, r^3 - r^2(4-\pi)\left[\frac{h}{2} - t - r\right] - W_{ps} \quad (3.23)$$

Where r is the internal radius of the corners to the hollow section

In the case of a circular hollow sections the W_{pc} can be determined from Eq. (3.24).

$$W_{pc} = \frac{(d-2t)^3}{6} - W_{ps} \quad (3.24)$$

Eq. (3.25) used for both type of sections (rectangular and circular).

$$h_n = \frac{A_C\, f_{cd} + f_{cd}}{2b f_{cd} + 4t\left(2f_{yd} - f_{cd}\right)} \quad (3.25)$$

For rectangular hollow sections, it can explain explicitly stated that by Eqs. (3.26) and (3.27).

$$W_{pan} = 2t{h_n}^2 \quad (3.26)$$

$$W_{pcn} = (b-2t){h_n}^2 - W_{psn} \quad (3.27)$$

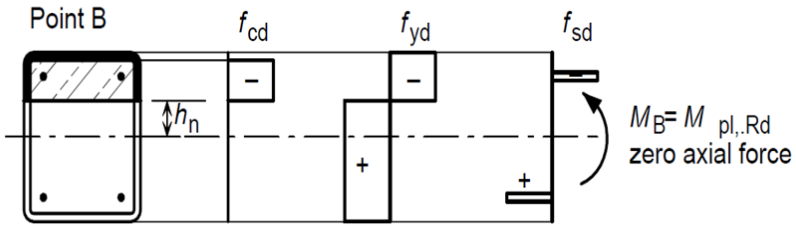

Figure 3.11 Stress distribution with point (B) on the interaction curve of concrete filled hollow cross section at $N_b = 0$ (Twilt et al. 1994).

At point (C) as shown in Figure 3.12, the axial compression and moment resistance of the composite column are given as Eq. (3.25) and (3.26), respectively.

$$N_c = N_{pm,Rd}\ (or\ N_{c,Rd}) = A_c f_{cd} \tag{3.25}$$

$$M_c = M_{pl,Rd} \tag{3.26}$$

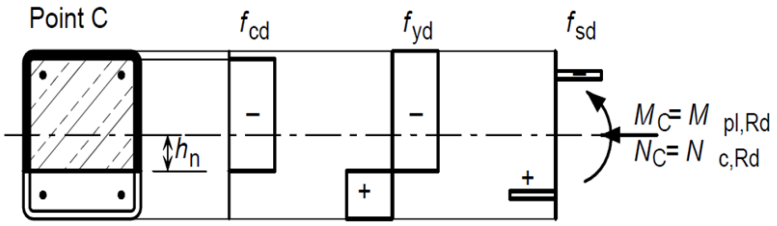

Figure 3.12 Stress distribution with point (C) on the interaction curve of concrete filled hollow cross section (Twilt et al. 1994).

At point (D) as shown in Figure 3.13, the plastic neutral axis coincides with the centroid of the cross-section, and the resulting axial force is half of the value at point C. $N_D = \frac{N_{pm,Rd}}{2}$, and $M_D = M_{max,Rd}$

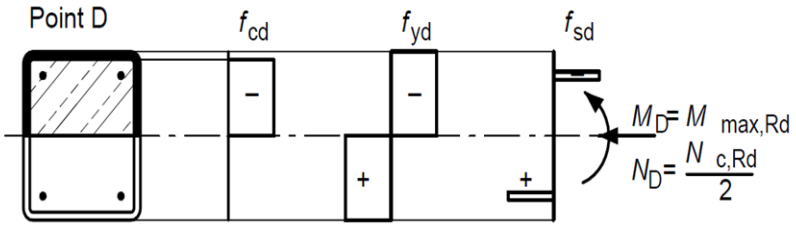

Figure 3.13 Stress distribution with point (D) on the interaction curve of concrete filled hollow cross section (Twilt et al. 1994).

Point (E) as shown in Figure 3.14, is halfway between A and C and is often required for highly non-linear interaction curves, in order to achieve a better approximation. In the case of a hollow section of concrete filled structure, the use of point E will yield a more economical design. However, much more calculation effort is required.

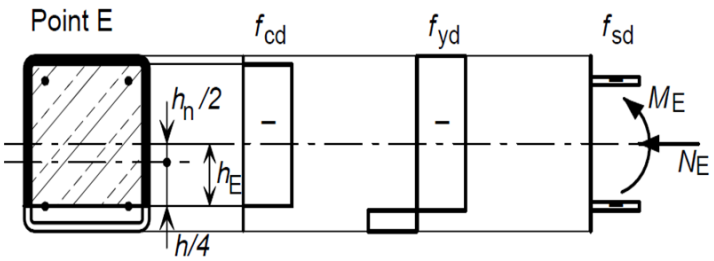

Figure 3.14 Stress distribution with point (E) on the interaction curve of concrete filled hollow cross section (Twilt et al. 1994).

3.3.4 Effective flexural stiffness, steel contribution ratio and relative slenderness

The steel contribution ratio δ should fulfil the following condition $0.2 \leq \delta \leq 0.9$ and calculated by Eq. (3.27).

$$\delta = \frac{A_a f_{yd}}{N_{pI,Rd}} \tag{3.27}$$

The relative slenderness $\overline{\lambda}$ should fulfil the following condition $\overline{\lambda} \leq 2{,}0$ and calculated by Eq. (3.28).

$$\overline{\lambda} = \sqrt{\frac{N_{pl,Rk}}{N_{cr}}} \tag{3.28}$$

Where: $N_{pl,Rk}$ is a plastic resistance of the composite section to compressive normal force, can be determined by Eq. (3.29).

$$N_{pl,Rk} = A_a f_y + A_c f_{ck} \tag{3.29}$$

N_{cr} is elastic critical normal force for the relevant buckling mode, calculated with the effective flexural stiffness $(EI)_{eff}$, can be determined by Eq. (3.30)

$$N_{cr} = \frac{\pi^2 (EI)_{eff}}{l^2} \tag{3.30}$$

For the determination of the relative slenderness $\bar{\lambda}$ and the elastic critical force N_{cr}, the characteristic value of the effective flexural stiffness $(EI)_{eff}$ of a cross-section of a composite column should be calculated from Eq. (3.31).

$$(EI)_{eff} = E_a I_a + k_e E_{cm} I_c \tag{3.31}$$

Where: E_a is modulus of elasticity of structural steel (210 000 N/mm^2), I_a is second moment of area of the structural section, k_e is a correction factor that should be taken as 0.6, E_{cm} is the secant modulus of elasticity of concrete, and I_c is the second moment of area of the un-cracked concrete section.

3.3.5 Column buckling resistance

The plastic resistance to compression of a composite cross-section $N_{pl,Rd}$ represent the maximum load that can be applied to column. The buckling resistance of a column is expressed as a proportion of the reduction factor (χ) of the plastic resistance to compression. The reduction factor can be determined from Eq. (3.32).

$$\chi = \frac{1}{\phi + \left[\phi^2 - \bar{\lambda}^2\right]^{0.5}} \leq 1.0 \tag{3.32}$$

Where: ϕ is the creep coefficient can be determined from Eq. (3.33).

$$\phi = 0.5\left[1 + \alpha\left(\bar{\lambda} - 0.2\right) + \bar{\lambda}^2\right] \tag{3.33}$$

Where: α is an imperfection factor depending on the buckling curve considered for rectangular hollows filled with concrete $\alpha = 0.21$, and for circular hollows filled with concrete $\alpha = 0.34$. The relevant buckling curve of the cross-section of the composite column is shown in Table 3.7.

The resistance of a composite column in axial compression (buckling load) is obtained from Eq. (3.34).

$$N_{pl,Rd} = \chi . N_{pl,Rd} \tag{3.34}$$

Table 3.7 Buckling curves and member imperfections for composite columns

Cross-section	Limits	Axis of buckling	Buckling curve	Member imperfection
concrete encased section 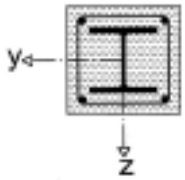		y-y	b	*L*/200
		z-z	c	*L*/150
partially concrete encased section 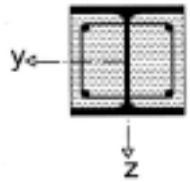		y-y	b	*L*/200
		z-z	c	*L*/150
circular and rectangular hollow steel section 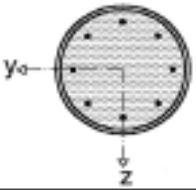	$\rho_s \leq 3\%$	any	a	*L*/300
	$3\% < \rho_s \leq 6\%$	any	b	*L*/200
circular hollow steel sections with additional I-section 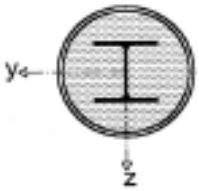		y-y	b	*L*/200
		z-z	b	*L*/200
partially concrete encased section with crossed I-sections 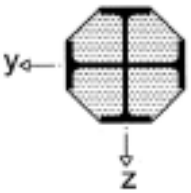		any	b	*L*/200

CHAPTER 4

RESULTS AND DISCUSSIONS

4.1 Verification of the Results

For the purpose of verification of the results both axial load and bending moment capacities are calculated using the two available codes AISC360-10 and EC4-2004, then they are compared with those mentioned in the published literature. Some samples were selected to validation of the results.

4.1.1 Verification of AISC360-10 results

The AISC360-10 results were verified by comparing them with those published in the literature review. Some sample sizes were taken as that of the paper. Values of axial load and bending moment capacities results are shown in Tables 4.1 and 4.2.

Table 4.1 Verification of columns according to AISC360-10 results

References	Cross-Sectional Properties					Material Properties		P_n	$AISC$ P_n
	L (mm)	H (mm)	B (mm)	t (mm)	b/t	f_c' (MPa)	f_y (MPa)	(kN)	(kN)
Kang et al. (2001)	749.3	249.9	249.9	3.2	76	24.8	317.9	2001	2001
	899.2	300	300	3.2	91	24.8	317.9	2297	2297
	899.2	300	300	3.2	91	30.3	317.9	2632	2632
Schneider (1998)	600	76.6	152.3	3	48	30.5	430	806	805
Uy (1998)	558	186	186	3	60	32	300	1507	1503
Lin (1998)	800	150	200	2.1	93	22.5	248.3	739	740
	800	150	150	1.4	105	35.3	247.3	653	653
	480	150	200	1.4	140	33.7	247	766	766
	800	150	200	2.1	93	35.3	248.3	984	983
	800	150	150	1.4	105	22.5	247.3	468	467
Anslijin and Janss (1974)	1318	329.9	329.9	4.47	71	31.6	370.3	4273	4273
	1328	331	331	4.47	72	27.4	370.3	3979	3979

As shown in Table 4.1. The AISC360-10 was used to calculated of axial load capacity. The results were almost similar to that done by Kang et al. (2001), Schneider (1998), Uy (1998), Lin (1998), and Anslijin and Janss (1974).

Table 4.2 Verification of beams according to AISC360-10 results

References	Cross-Sectional Properties					Material Properties		M_n $(kN.m$	$AISC$ M_n $(kN.m)$
	L (mm)	H (mm)	B (mm)	t $(mm$	b/t	f_c' $(MPa$	f_y (MPa)		
Han et al. (2006)	1400	200	200	1.9	103.3	54.5	282	32.9	32.9
Jiang et al. (2013)	2000	150	150	2.0	73	56	397	26.3	26.3

As shown in Table 4.2. The AISC360-10 was used to calculated of bending moment capacity. The results were almost similar to that done by Han et al. (2006) and Jiang et al. (2013).

4.1.2 Verification of EC4-2004 results

The EC4-2004 results were verified by comparing them with those published in the literature review. Some sample sizes were taken as that of the paper. Values of axial load and bending moment capacities results are shown in Tables 4.3 and 4.4.

Table 4.3 Verification of columns according to EC4-2004 results

References	Cross-Sectional Properties					Material Properties		N (kN)	$EC4$ N (kN)
	L (mm)	H (mm)	B (mm)	t (mm)	b/t	f_{ck} $(MPa$	f_y (MPa)		
Uy et al. (2011)	440	103	103	2.76	35.3	36.3	390	746	746
	440	103	103	2.76	35.3	75.4	390	1096	1097

As shown in Table 4.3. The EC4-2004 was used to calculated of axial load capacity. The results were almost to that done by Uy et al. (2011).

Table 4.4 Verification of beams according to EC4-2004 results

References	Cross-Sectional Properties					Material Properties		M_n $(kN.m$	$EC4$ M_n $(kN.m)$
	L (mm)	H (mm)	B (mm)	t (mm)	b/t	f_{ck} $(MPa$	f_y (MPa)		
Arivalagan and Kandasamy (2010)	1000	100	50	3.2	13.6	37	338	10.1	10
	1000	100	50	3.2	13.6	35	338	10	9.96
	1000	100	50	3.2	13.6	21.6	338	9.9	9.7
Han (2004)	1100	120	120	5.86	18.5	26.3	330.1	39.8	40
	1100	120	120	5.86	18.5	22	330.1	39	39

As shown in Table 4.4. The EC4-2004 was used to calculated bending moment capacity. The results were almost similar to that done by Arivalagan and Kandasamy (2010) and Han (2004).

4.2 Parametric study

The concentration on the investigation of which parameters effect on the design of RCFST members and also used various codes to compute their axial load and bending moment capacities. The codes are as follows:

- EC4-2004
- AISC360-10.

The first is to develop a spreadsheet using Microsoft Excel for each one of the design codes to compute the axial load and bending moment capacities of RCFST members.

Then the obtained results from the spread sheet will be verified and compared with previous studies mentioned in Chapter 2.

Finally, the effect of the mentioned parameters on both axial load and bending moment capacity will be calculated as well as the parameters which have greater impact will be determined.

$H, B, t, f_c', and\ f_y$ are input data to be analyzed by the General Linear Model (GLM) method for beam and column. The height of the rectangular cross-section (H) begins between 25 to 260 (mm), the width of rectangular cross-section (B) begins between

25 to 260 (mm), the thickness of the steel tube (t) begins between 1.5 to 10 (mm) and the constant column length $L = 3000(mm)$, all data according to British Standard (BS EN.10219-2:2006) codes and production ranges (blue color) were used as shown in Table A1, and the limitation for f_c' (20,30,40,50 and 60) MPa and f_y (235,275 and 355) MPa were chosen from EC4-2004 and AISC360-10, and 8520 different analysis carried out for each code and model of beams and columns. In order to find out the important parameters that influence the axial load and bending moment capacities.

4.3 Results and Discussion

A total of 8520 different sections were studied. The axial load and bending moment capacity of these were calculated based on the rules issued by both AISC360-10 and EC4-2004.

For the purpose of investigation of which parameters has greater effect on both axial load and bending moment capacity, a GLM method which is a statistical method was used for the purpose of analysis. For the all sections used in the study, different parameters including section's (height, width, thickness, yield stress of steel and compressive strength of concrete) were studied at different values which mainly led to have different axial load and bending moment values.

By using the GLM, the effect of the tested parameters on both axial load and bending capacity were calculated and the greater impact among those parameters were recorded. Tables 4.5 and 4.6 shows final results obtained from the analysis based on both codes.

Table 4.5 The effect of the parameters on axial load capacities with respect to design codes for columns ($L = 3000mm$)

Model Term	AISC360-10		EC4-2004	
	Quantity contributions	Order	Quantity contributions	Order
$H(mm)$	0.723	1	0.515	1
$B\ (mm)$	0.226	2	0.312	2
$t\ (mm)$	0.001	5	0.074	3
$f_y\ (Mpa)$	0.017	4	0.050	4
$f_c'\ (Mpa)$	0.032	3	0.049	5

As shown in the Table 4.5, (H) parameter, has the greater impact on axial load in both codes. (B) parameter, has the second greater impact on axial load in both codes. (t) parameters have greater impact in EC4-2004 when compared to AISC360-10, (f_y) has the same impact in both codes. Finally, in term of (f_c'), it has the greater impact on column according to AISC360-10 when compared to EC4-2004.

Therefore, based on the results mentioned above, when choosing a section for column, designers and engineers should put more consideration on the section height and width respectively in order to have more axial load capacity on columns.

Table 4.6 The effect of the parameters on bending moment capacities with respect to design codes for beams.

Model Term	AISC360-10		EC4-2004	
	Quantity contributions	Order	Quantity contributions	Order
$H(mm)$	0.860	1	0.794	1
$B\ (mm)$	0.072	2	0.066	3
$t\ (mm)$	0.010	4	0.043	4
$f_y\ (Mpa)$	0.058	3	0.097	2
$f_c'\ (Mpa)$	0.001	5	0.000	5

As shown in the Table 4.6, all the studied parameters have an effect on beams, however they are ranging according to the codes used.

(H) parameter, has the greater impact on bending moment in both codes while (f_c') mostly has the less impact. (B) parameter, has the second greater impact on bending moment according to AISC360-10, while it has third greater impact according to EC4-2004, (t) parameters have the same impact in both codes, finally (f_y) has greater impact according to EC4-2004 when compared to AISC360-10.

Therefore, based on the results mentioned above, when choosing a section for beam, designers and engineers should put more consideration on the section height and width respectively in order to have more bending moment capacity.

CHAPTER 5

CONCLUSION

5.1 Conclusion

In this research, the compressive capacity of the RCFST columns and beams under axial loads and bending moment capacities was investigated. Two codes were adopted in this study including the EC4-2004 and AISC360-10 are investigated to estimate the compressive capacity of RCFST columns and beams. The design according to standards is based on finding the capacity subjected to axial load and bending moment capacities. The steps used to design the column and beam using the standards are explained in detail in separate chapters. The equations to summarize the design steps and to make it easier for the reader to understand the equations used. In addition to the design of the RCFST column and beam manually, a spreadsheet solver was developed using Microsoft Excel software for the two standards. The spreadsheet solver helps the user to design and check the safety of any section of RCFST column and beam, by inserting few input parameters.

There are several factors that affect the capacity of the RCFST beams and columns. Geometrical and material properties such as cross-sectional shape (H, B, t), steel yield strength (f_y), and concrete compressive strength (f_c').

- According to the requirements of AISC360-10, and EC4-2004 after comparing the effect of parameters can be concluded that the main parameter which effects on axial load and bending moment capacity were the height (H) of rectangular beam which were equal to (86%) and for column equal to (72.3%) according to AISC360-10, and for EC4-2004 for beam and column equal to (79.4%) and (51.5%), respectively. The (H) of columns and beams are very critical parameter that must be considered in the structural designing process.

- Specially f_c' which had very small effected on the axial load and bending moment capacities according to AISC 360-10 and EC4-2004. But, it has an effect of filling concrete in hollow sections is increasing capacity versus hollow sections.
- Columns height and width are different contributions of design codes. These differences are based on the accounting confinement of concrete.
- Preliminary design RCFST beam and columns deciding the height of the column or beam is a most important key point for a design engineer.
- The comparison between the various codes AISC 360-10 and EC4-2004 results were performed with respect to many factors. Some of them were capacity of the section, cost, accuracy of results and equations used.

5.2 Recommendations for future works

In general, the research area can be expanded, by taking in consideration other aspects which may be beneficial in achieving effective design. The following aspects can be taken in other studies in order to improve or solve the problems that might be arisen when designing both beam and column sections:

1. For the purpose of optimizing the axial load and bending moment capacity, it's possible to include other standards rather than American and European code such as: Australian code, Canadian code, Chinese code, Japanese code etc.

2. It recommended to study other types of composite columns and beams, such as circular hollow section, concrete encased sections, and partially encased concrete sections.

3. It's also suggested to include the study of shear connectors impacts on the design of CFST beams and columns.

4. Including reinforcement in the design is also recommended.

5. Finally, it's also suggested to perform an economical study in order to determine the most economical section for a given load.

REFERENCES

Abdalla, S. H. (2012). Behavior of concrete filled steel tube (CFST) under different loading conditions. American University of Sharjah.

Arivalagan, S.& Kandasamy, S. (2010). Finite element analysis on the flexural behaviour of concrete filled steel tube beams. *Journal of Theoretical and Applied Mechanics*, **48(2)**, 505-516.

Anslijn, R., & Janss, J. (1974). Le calcul des charges ultimes des colonnes métalliques enrobées de béton. Centre de Recherches Scientifiques et Techniques de l'Industrie des Fabrications Métalliques.

AISC 360-10. (2010). Specification for Structural Steel Buildings. (ANSI/AISC 360-10). American Institute of Steel Construction. Chicago-Illinois.USA.

British Standard BS EN.10219-2: 2006. Cold Form Welded Structural Hollow Section of Non-alloy and Fire Grain Steels-Part 2: Tolerance, dimension and sectional properties.

Chen, C. C., & Lin, N. J. (2006). Analytical model for predicting axial capacity and behavior of concrete encased steel composite stub columns. *Journal of Constructional Steel Research*, **62(5)**, 424-433.

Choi, K. K. (2007). Analytical and experimental studies on mechanical behavior of confined concrete filled tubular columns. University of Southern California.

Choi, Y. H. (2004). A Modified AISC P-M Interaction Curve for Square Concrete Filled Tube Beam-Columns. University of Illinois at Urbana-Champaign.

Choi, Y. H., Foutch, D. A., & LaFave, J. M. (2006). New approach to AISC P–M interaction curve for square concrete filled tube (CFT) beam–columns. *Engineering structures*, **28(11)**, 1586-1598.

Eurocode. (2004). Eurocode 4 : Design of Composite Steel and Concrete Structures Part 2 : General Rules And Rules For Buildings. CEN, Brussels, Belgium, 1–117.

Elchalakani, M., Zhao, X. L., & Grzebieta, R. H. (2001). Concrete-filled circular steel tubes subjected to pure bending. *Journal of constructional steel research*, **57(11)**, 1141-1168.

Ellobody, E., Young, B., & Lam, D. (2006). Behaviour of normal and high strength concrete-filled compact steel tube circular stub columns. *Journal of Constructional Steel Research,* **62(7)**, 706-715.

Fanning, P. J., & Kelly, O. (2001). Ultimate response of RC beams strengthened with CFRP plates. *Journal of Composites for Construction,* **5(2)**, 122-127.

Furlong, R. W. (1967). Strength of steel-encased concrete beam columns. *Journal of the Structural Division,* **93(5)**, 113-124.

Gardner, N. J., & Jacobson, E. R. (1967). Structural behavior of concrete filled steel tubes. *In Journal Proceedings,* **64(7)**, 404-413.

Ghannam, S. (2016). Flexural strength of concrete-filled steel tubular beam with partial replacement of coarse aggregate by granite. *International Journal of Civil Engineering and Technology (IJCIET),* **7**, 161-168.

Gourley, B. C., Tort, C., Hajjar, J. F., & Schiller, P. H. (2001). A synopsis of studies of the monotonic and cyclic behaviour of concrete-filled steel tube beam-columns. University of Minnesota.

Grauers, M. (1993). Composite columns of hollow steel sections filled with high strength concrete . Chalmers University of Technology.

Guler, S., Copur, A., & Aydogan, M. (2012). Flexural behaviour of square UHPC-filled hollow steel section beams. *Structural Engineering and Mechanics,* **43(2)**, 225-237.

Gupta, P. K., Sarda, S. M., & Kumar, M. S. (2007). Experimental and computational study of concrete filled steel tubular columns under axial loads. *Journal of Constructional Steel Research,* **63(2)**, 182-193.

Han, L. H. (2004). Flexural behaviour of concrete-filled steel tubes. *Journal of Constructional Steel Research,* **60(2)**, 313-337.

Han, L. H., Lu, H., Yao, G. H., & Liao, F. Y. (2006). Further study on the flexural behaviour of concrete-filled steel tubes. *Journal of Constructional Steel Research,* **62(6)**, 554-565.

Han, L. H., Yao, G. H., & Zhao, X. L. (2004). Behavior and calculation on concrete-filled steel CHS (circular hollow section) beam-columns. *Steel and Composite structures,* **4(3)**, 169-188.

Jiang, A. Y., Chen, J., & Jin, W. L. (2013). Experimental investigation and design of thin-walled concrete-filled steel tubes subject to bending. *Thin-Walled Structures*, **63**, 44-50.

Kang, C. H., Shin, K. J., Oh, Y. S., & Moon, T. S. (2001). Hysteresis behavior of CFT column to H-beam connections with external T-stiffeners and penetrated elements. *Engineering structures*, **23(9)**, 1194-1201.

Kawaguchi, J., Morino, S., Shirai, J., and Tatsuta, E. (1998). Database and structural characteristics of CFT beam-columns. *Proceedings of the Fifth Pacific Structural Steel Conference, Seoul, Korea.*

Knowles, R. B., & Park, R. (1969). Strength of concrete filled steel columns. *Journal of the structural division*.

Kuranovas, A., Goode, D., Kvedaras, A. K., & Zhong, S. (2009). Load-bearing capacity of concrete-filled steel columns. *Journal of civil engineering and management*, **15(1)**, 21-33.

Lai, Z. (2014). Experimental database, analysis and design of noncompact and slender concrete-filled steel tube (CFT) members. Purdue University.

Lai, Z., Varma, A. H., & Griffis, L. G. (2015). PM interaction equations for design of CFT beam-columns. *Structures Congress 2.*

Lam, D., & Gardner, L. (2008). Structural design of stainless steel concrete filled columns. *Journal of Constructional Steel Research*, **64(11)**, 1275-1282.

Liew, J. R., & Xiong, D. X. (2012). Ultra-high strength concrete filled composite columns for multi-storey building construction. *Advances in Structural Engineering*, **15(9)**, 1487-1503.

Lu, F. W., Li, S. P., & Sun, G. (2007). A study on the behavior of eccentrically compressed square concrete-filled steel tube columns. *Journal of Constructional Steel Research*, **63(7)**, 941-948.

Lai, Z., Varma, A. H., & Zhang, K. (2014). Noncompact and slender rectangular CFT members: Experimental database, analysis and design. *Journal of Constructional Steel Research*, **101**, 455-468.

Lu, Y. Q., & Kennedy, D. L. (1994). The flexural behaviour of concrete-filled hollow structural sections. *Canadian Journal of Civil Engineering*, **21(1)**, 111-130.

Lin, C. Y. (1988). Axial capacity of concrete infilled cold-formed steel columns.

MacGregor, J. G. (1992). Reinforced concrete: Mechanics and design.

Mursi, M., & Uy, B. (2004). Strength of slender concrete filled high strength steel box columns. *Journal of Constructional Steel Research,* **60(12)**, 1825-1848.

O'Shea, M. D., & Bridge, R. Q. (2000). Design of circular thin-walled concrete filled steel tubes. *Journal of Structural Engineering,* **126(11)**, 1295-1303.

Perea, T., & Leon, R. (2011). Behavior of composite CFT beam-columns based on nonlinear fiber element analysis. *In Composite Construction in Steel and Concrete*, 237-251.

Roeder, C. W., Lehman, D. E., & Bishop, E. (2010). Strength and stiffness of circular concrete-filled tubes. *Journal of structural engineering,* **136(12)**, 1545-1553.

Sakino, K., Tomii, M., & Watanabe, K. (1985). Sustaining load capacity of plain concrete stub columns by circular steel tubes. *International Special Conf. on Concrete-filled Steel Tubular Structure,* 112-118.

Schiller, P. H., Hajjar, J. F., & Gourley, B. C. (1994). Expressions for the Elastic Rigidity of Rectangular Concrete-Filled Steel Tube Beam-Columns. *Structural Engineering Report No. ST-94-2,* Department of Civil Engineering, University of Minnesota, Minn.

Schneider, S. P. (1998). Axially loaded concrete-filled steel tubes. *Journal of structural Engineering,* **124(10)**, 1125-1138.

Tomii, M., & Sakino, K. (1979). Elasto-plastic behavior of concrete filled square steel tubular beam-columns. *Transactions of the Architectural Institute of Japan*, no. **280**, pp. 111-120.

Tomii, M., Yoshimura, K., & Morishita, Y. (1977). Experimental studies on concrete-filled steel tubular stub columns under concentric loading. ASCE.

Tort, C., & Hajjar, J. F. (2007). Reliability-based performance-based design of rectangular concrete-filled steel tube (RCFT) members and frames. University of MinnesotaMajor: Civil engineering.

Twilt, L., Hass, R., Klingsch, W., Edwards, M., & Dutta, D. (1994). Design guide for structural hollow section columns exposed to fire. Verlag TÜV Rheinland.

Uy, B., Tao, Z., & Han, L. H. (2011). Behaviour of short and slender concrete-filled stainless steel tubular columns. *Journal of Constructional Steel Research,* **67(3)**, 360-378.

Uy, B. (1998). Local and post-local buckling of concrete filled steel welded box columns. *Journal of Constructional Steel Research,* **47(1-2)**, 47-72.

Vijay laxmi B. V., Manoj Kumar Chitawadagi. (2014). Finite Element Analysis of Concrete Filled Steel Tube (CFT's) Subjected to Flexure. *International Journal of Engineering Inventions*, **3(12)**, 18-28.

Wang, R., Han, L. H., Nie, J. G., & Zhao, X. L. (2014). Flexural performance of rectangular CFST members. *Thin-Walled Structures*, **79**, 154-165.

Xiamuxi, A., & Hasegawa, A. (2011). Experimental study on reinforcement ratio of RCFT columns under axial compression. *In Advanced Materials Research*, **250**, 3790-3797.

Zhang, W., & Shahrooz, B. M. (1999). Comparison between ACI and AISC for concrete-filled tubular columns. *Journal of Structural Engineering*, **125(11)**, 1213-1223.

Zubydan, A. H., & ElSabbagh, A. I. (2011). Monotonic and cyclic behavior of concrete-filled steel-tube beam-columns considering local buckling effect. *Thin-Walled Structures*, **49(4)**, 465-481.

APPENDIX

Appendix A: Parameters shapes

Table A1. Parameters used for calculating axial load and bending moment capacities according to production range in (BS EN 10219) code

	Wall Thickness (mm)															
mm	1.5	2.0	2.5	3.0	3.5	4.0	4.5	5.0	5.5	6.3	6.5	7.0	8.0	9.0	9.5	10.0
25x25																
30x20																
40x10																
30x30																
20x40																
50x10																
35x25																
40x30																
20x50																
35x35																
40x40																
30x50																
20x60																
50x50																
40x60																
70x30																
80x20																
60x50																
80x30																

40x80																
30x90																
50x70																
60x60																
70x70																
60x80																
50x90																
40x100																
75x75																
70x80																
60x90																
50x100																
80x80																
70x90																
60x100																
40x120																
90x90																
80x100																
60x120																
40x140																
75x125																
80x120																
100x100																
100x120																
80x140																
80x160																
120x120																
100x150																
90x160																

125x125																
100x160																
120x140																
140x140																
120x160																
80x200																
100x200																
125x175																
140x160																
150x150																
100x250																
150x200																
175x175																
150x250																
100x300																
200x200																
150x350																
200x300																
250x250																
200x320																